Dear author,

Please note that changes made in the online proofing system will be added to the article before publication but are not reflected in this PDF.

We also ask that this file not be used for submitting corrections.

Commun Nonlinear Sci Numer Simulat xxx (xxxx) xxx

Contents lists available at ScienceDirect

Commun Nonlinear Sci Numer Simulat

journal homepage: www.elsevier.com/locate/cnsns

Research paper

Size-dependent nonlinear forced vibration and dynamic stability of electrically actuated micro-plates

Q2 I. Karimipour[a,b], Y. Tadi Beni[a,*], A.H. Akbarzadeh[a,c]

[a] Department of Mechanical Engineering, Shahrekord University, Shahrekord, Iran
[b] AML Laboratory, Department of Bioresource Engineering, McGill University, Island of Montreal, QC H9X3V9 Canada
[c] Department of Mechanical Engineering, McGill University, Montreal, QC H3A 0C3 Canada

ARTICLE INFO

Article history:
Received 23 February 2019
Revised 11 May 2019
Accepted 21 May 2019
Available online xxx

Keywords:
Micro-electromechanical plate
Dynamic pull-in instability
Modified couple stress theory
Multiple scale method

ABSTRACT

A size-dependent structural dynamic model that incorporates the effect of geometric nonlinearity is developed in this paper for the forced vibration, and dynamic stability of thin rectangular micro-plates. The equations of motion for micro-plates are derived within the framework of classical plate theory, modified couple stress theory (MCST), and von Kármán geometric nonlinearity using Hamilton's principle. Galerkin method is used to convert the governing partial differential equations to a nonlinear second-order ordinary differential equation, which is solved by a Runge-Kutta method. The static instability analysis of the micro-plate is performed to determine the critical electrostatic voltages, and to avoid the pull-in instability. By tracking the static behavior of the microplate, and determining the electrostatic pull-in voltage, the frequency response curves are plotted. In dynamic response, primary, superharmonic, and subharmonic resonance are studied, and the frequency response equation is obtained for each case by the method of multiple scales. Further efforts are made to investigate the influence of size effect, electrical loading (DC and AC voltages), and excitation frequency on the static, and dynamic responses, critical AC voltages, and dynamic stability of micro-plates. It is found that the critical dynamic voltage is a function of the frequency of excitation force. It is shown that the stiffness of micro-plate decreases by increasing the constant DC voltage; however, the increase in the alternating AC voltage does not considerably affect the stiffness of the micro-plate.

1. Introduction

Recent studies show that electrically-actuated micro-plates have a vast range of applications in microelectromechanical systems (MEMS) as actuation components in micro-pumps, micro-mirrors, microphones, micro-switches, and micro-sensors [1–6]. The actuation force can be applied to the micro-plates in the form of electrical, magnetic and thermal excitation, so-called as multi-physical stimuli [3,7–10]. In the case of electrical actuation, an electrically-actuated micro-plate is formed by a variable capacity air-gap capacitor on one side and a stationary electrode connected to the output circuit on the other side [11,12]. Electrostatic actuators contain two conductive electrodes, one movable and one fixed (grounded). Applying a voltage between the electrodes leads to the deflection of the movable electrode toward the fixed electrode [13,14]. Many studies in the literature, however, have overlooked the bending stiffness and modelled the plate as a membrane element [1,11,15–19].

* Corresponding author.
E-mail address: tadi@eng.sku.ac.ir (Y.T. Beni).

https://doi.org/10.1016/j.cnsns.2019.104856
1007-5704/

Many researchers have investigated the behavior of electrically-stimulated micro-beams in resonator sensors. These studies have fallen into two categories. The first category focused on the static behavior of micro-beams bent by a DC electrostatic force. The second category studied the vibration behavior of micro-beams by a harmonic AC voltage. Zook et al. [20] considered micro-plates and micro-beams and calculated their fundamental frequencies using a finite element method. The natural frequencies obtained by the finite element method were higher than the measured natural frequencies measured by experimental tests. Choi and Lovell [21] calculated the static deformation of a micro-beam using a numerical integration scheme and a shooting method. Their models included electrostatic force and mid-plane stretching. Ahn et al. [22] modeled an electrically-driven micro-beam as one degree of freedom mass-spring-damper system. They used this model to obtain an analytical expression for the fundamental natural frequency as a function of constant DC voltage. The second category of research was initiated by Zook et al. [20]. They showed that increasing the AC voltage increases the resonance frequency (hardening behavior). Tilmans and Legtenberg [23] studied the dynamic problem of the system for the large values of the AC voltage using the Rayleigh-Ritz energy method, taking into account the electric forces and the stretchability of the mid-plane. Ayela and Fournier [24] studied the response of micro-beams with different geometric shapes under a total electrical excitation including DC and AC voltages. They plotted different diagrams to show the variation of resonant frequency relative to the excitation amplitude for different axial loads. Laboratory results showed that some of the micromachined silicon resonators have a softening behavior for the operating conditions. While others have a hardening behavior, they concluded that a nonlinear behavior might be due to different phenomena, e.g., the mechanical properties of these resonators. Veijola et al. [25] modeled a micro-beam using a nonlinear mass and spring model of order three, which includes the stretch of the intermediate plane. Using the Harmonic Balance Method, they showed that a nonlinear term caused by electrical force leads to a softening behavior, while the stretching of the mid-plane results in a hardening behavior.

Pull-in instability in micro-electromechanical devices is investigated by Konig and Wachutka [26]. This instability occurs when the input voltage trespasses a critical value called the pull-in voltage [27]. In this way, the elastic restoring force of the movable electrode cannot resist the Coulomb attraction force, and this electrode abruptly adheres to the fixed one. Ng et al. [28] have studied the characteristics of an electrically stimulated plate. The governing Laplace equation is solved by the boundary element method. Also, the nonlinear geometric factors related to the tension of the mid-plane are included in the plate model. Subsequently, electromechanical coupling equations were solved by the repetition method. Significant qualitative differences were observed between the results of the linear and nonlinear analysis for large plate deformations. Zhao et al. have studied nonlinear modeling of simply supported rectangular plates [29]. They determined static deformation using a numerical shooting method and a reduced order method. They also studied the mechanical behavior of rectangular plates under electrical excitation. The linear and nonlinear vibration of plates have been studied by a large number of researchers. Analytical methods, along with numerous numerical theories, have been widely used in practice [30].

After the dimensions have reduced to a sub-micron scale, the nano-scale phenomena emerge, which should be taken into account in establishing the theoretical models [31,32]. One of the major critical instances of the nano-scale phenomenon is the size-dependency of the mechanical performance of nanostructures, which appears in the deformation tests of microstructures [33]. Due to the fact that the materials at the atomic scale are naturally discrete, the classical continuum mechanics are supposed to be insufficiently effective for modeling the size-dependent behavior of them at sub-micron distances. The ever-increasing progress in micro-structure materials leads to extending the usages of higher-order continuum theories. In constructing a large number of devices in a nano-scale, the classical elasticity, due to neglect size effect, loses its efficiency [34]. In the past decades, the researchers and experts have extensively and particularly adopted higher-order continuum theories in the nano-scale studies of thin films, nano-composites, and quantum dots. Employing the classical continuum theory in the problems which encompass thin films, nano-composites, and quantum dots, yielded extremely unexpected results [35]. Couple stress theory [36], non-local elasticity theory [37], micro-polar elasticity theory [38], strain gradient elasticity theory [39–42] and surface elasticity [43] are good instances of the theories developed and used to study the mechanical behaviors of micro-scale structures [31]. Modified couple stress theory introduces one material length scale parameter as an additional elastic constant to interpret the size-dependent behavior of elastic solids [44]. In the following, some of the works on the modified couple stress theory will be reviewed. Tsiatas [45] presented a size-dependent model for testing the static flexure of thin micro-plates based on assumptions Kirchhoff model. He concluded that in the smaller thickness of the micro-plate or the more significant amount of its material length to its thickness (l/h), the influence of size effect increases. Using the method presented by Tsiatas, Yin et al. [46] introduced the non-classic model of Kirchhoff's plate to investigate the effect of size on the first two natural frequencies of micro-plates based on modified couple stress theory. Also, Jomehzadeh et al. [47] using the model provided by Tsiatas, analytically investigated the effect of size on the natural frequency of thin simply supported micro-plates based on modified couple stress theory and Kirchhoff assumptions. They also examined circular plates with different boundary conditions. They showed that by decreasing the thickness of the micro-plates, the value of natural frequency significantly increased. Then Asghari [48] expanded Tsiatas's work by considering non-linear geometric effects in equations. He also presented the size-dependent model for thin plates by recognizing nonlinear geometric effects based on the modified couple stress theory. Wang et al. [49] presented a non-classical model for Kirchhoff plates based on the principle of minimum potential energy to analyze nonlinear bending micro-circular plates under a uniform load. The governing equations first were converted to nonlinear algebraic equations using Collocation point method, and then these equations were solved using the Newton- Raphson numerical method. Numerical results showed the plate that is modeled using MCST is stiffer than the plate is modeled using classical theory, so the lower ratio of thickness

Please cite this article as: I. Karimipour, Y.T. Beni and A.H. Akbarzadeh, Size-dependent nonlinear forced vibration and dynamic stability of electrically actuated micro-plates, Commun Nonlinear Sci Numer Simulat, https://doi.org/10.1016/j.cnsns.2019.104856

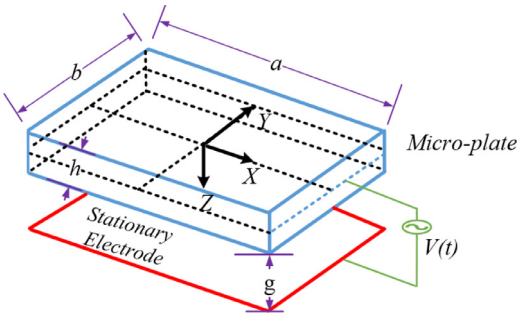

Fig. 1. Schematic figure of a rectangular micro-plate.

to the material length scale parameter, the difference between two theories gets bigger. Akgoz and Civalek [50] investigated an analytical solution for static bending, and free vibration of micro-plates rested on an elastic foundation based on modified couple stress theory. Equations were derived based on the Kirchhoff plate theory, and for solving equations, the Navier's method was used. Askari and Tahani [51] extracted the size-dependent natural frequency of thin-rectangular micro-plate with clamped boundary condition based on the modified couple stress theory using the extended Kantorovich method (EKM). They also [52] investigated the size effects on the natural frequencies in thin clamped micro-plates under the electrostatic field. They concluded that accounting the size effects in the free vibration analysis of pre-deformed micro-plate, under applying the electrical potential is more urgent than one with un-deformed structure. Tahani et al. [53] investigated the effects of length scale on natural frequencies and linear and un-damped mode shapes of thin rectangular micro-plates. The micro-plate has initial deflection under the presence of an electrostatic field. They used the finite element method to solve equations and showed that the convergence of results is gained by using a 20×20 grid of points. They concluded that the influence of the size effect on the natural frequencies of the pre-deformed plates when $h > 20l$ (thickness ratio to a material length scale) is negligible, while considering the size effect is essential for $h < 10l$. Zhang et al. [54] presented the size-dependent finite element model for thick Mindlin micro-plates using modified couple stress theory. They studied static bending, buckling, and free vibration of thick micro-plates using the finite element model. It should be noted that all the mentioned papers have been examined for homogeneous micro-plates. Recently, the modified couple stress theory is used to analyze the functionally graded micro-plate. A literature survey on these topics has been carried out in [55–59].

Due to the review carried out in previous studies in the field of the micro-plates, the main objective of this work is study on the nonlinear forced vibration and dynamic behavior of rectangular micro-plates under electrical excitation. To fill this gap, the present study adopts MCST components together with developing a semi-analytical method which is appropriate for studying the micro-plate's forced vibration. The applied excitation is made up of a constant current voltage DC and a variable AC voltage. In this analysis, the first step is to achieve the equations of motion under the electrical excitation and to simplify them. Then, to obtain the static response of the system under constant voltage (DC voltage), these equations are solved by different methods. By identifying the critical voltage and applying electrical excitation consisting of constant and alternating current voltages, the frequency response curves for the primary and secondary resonance modes are investigated. Other objectives of this study are to study the effects of electrical load parameters, (namely DC and AC driving voltages), and the influence of excitation frequency on the static and vibrational behavior of the micro-plate. In this regard, semi-analytical relations for static and vibration responses of the micro-plate under electrical stimulation are obtained, and critical voltage and the dynamic stability of the system are reported.

2. Size-dependent micro-plate model

The classical plate theory (CPT) is applied to plates whose thickness is small compared to other dimensions, where the transverse shear deformation, rotation inertia, and normal transverse stress can be neglected [60]. Fig. 1 demonstrates a schematic figure of a micro-plate, constructed of two conductive electrodes (one movable and one fixed (grounded)). The considered micro-plate has the length and width of a and b in the X and Y directions, while its thickness is h. The initial gap between the non-actuated micro-plate and the fixed substrate is assumed to be g. In addition, X, Y, and Z are the coordinates along the length, width, and thickness, respectively.

According to the underlying hypothesis of the classical thin micro-plate theory, the displacement field (U_1, V_1, W_1) of an arbitrary point of the micro-plate can be specified as [61]:

$$\begin{aligned} U_1(X,Y,Z,t) &= U(X,Y,t) - Z\frac{\partial}{\partial X}W(X,Y,t), \\ V_1(X,Y,Z,t) &= V(X,Y,t) - Z\frac{\partial}{\partial Y}W(X,Y,t), \\ W_1(X,Y,Z,t) &= W(X,Y,t) \end{aligned} \tag{1}$$

Please cite this article as: I. Karimipour, Y.T. Beni and A.H. Akbarzadeh, Size-dependent nonlinear forced vibration and dynamic stability of electrically actuated micro-plates, Commun Nonlinear Sci Numer Simulat, https://doi.org/10.1016/j.cnsns.2019.104856

where (U_1, V_1, W_1) are the corresponding displacements along with the (X, Y, Z) coordinates. In Eq. (1), U, V , $and W$ represent the mid-plane displacements along the coordinate directions.

Since the thickness of the micro-plate compared to other dimensions is assumed to be small, the classical plate theory is adopted in this research. The nonlinear analysis of the plates is of great importance when the amplitude of lateral vibration of the micro-plate is greater than the half of the thickness of the micro-plate, and therefore an essential nonlinear term should be considered in the governing equation. Due to the presence of a nonlinear geometric term, resonance frequencies and the mode shapes are dependent on the amplitude of lateral load. von Kármán equations which incorporate the effect of mid-plane stretch are widely used in the free and forced nonlinear vibration of plates [62]. Since later deformation is comparable to the thickness of micro-plates, classical plate theory is applied for a geometrically-nonlinear problem. For micro-plates with insignificant strains, moderate slopes, and large deflections, the non-zero strain components associated with the displacement field, based on the von Kármán equation, can be written as [61, 63, 64]:

$$\varepsilon_{ZZ} = \varepsilon_{XZ} = \varepsilon_{YZ} = 0,$$
$$\begin{Bmatrix} \varepsilon_{XX} \\ \varepsilon_{YY} \\ \gamma_{XY} \end{Bmatrix} = \begin{Bmatrix} {\varepsilon^0}_{XX} \\ {\varepsilon^0}_{YY} \\ {\gamma^0}_{XY} \end{Bmatrix} - Z \begin{Bmatrix} \frac{\partial^2 W}{\partial X^2} \\ \frac{\partial^2 W}{\partial Y^2} \\ 2\frac{\partial^2 W}{\partial X \partial Y} \end{Bmatrix}, \quad \begin{Bmatrix} {\varepsilon_{XX}}^{(0)} \\ {}^{(0)}_{\varepsilon_{YY}} \\ {\gamma^{(0)}}_{XY} \end{Bmatrix} = \begin{Bmatrix} \frac{\partial U}{\partial X} + \frac{1}{2}\left(\frac{\partial W}{\partial X}\right)^2 \\ \frac{\partial V}{\partial Y} + \frac{1}{2}\left(\frac{\partial W}{\partial Y}\right)^2 \\ \frac{\partial U}{\partial Y} + \frac{\partial V}{\partial X} + \frac{\partial W}{\partial X}\frac{\partial W}{\partial Y} \end{Bmatrix} \tag{2}$$

The non-zero components of the rotation vector and curvature tensor, associated with the displacement field presented in Eq. (1), can also be written as:

$$\begin{Bmatrix} \theta_{XX} \\ \theta_{YY} \\ \theta_{ZZ} \end{Bmatrix} = \frac{1}{2} Curl \begin{Bmatrix} U_1 \\ V_1 \\ W_1 \end{Bmatrix} = \begin{Bmatrix} \frac{1}{2}\left(\frac{\partial W_1}{\partial Y} - \frac{\partial V_1}{\partial Z}\right) \\ \frac{1}{2}\left(\frac{\partial U_1}{\partial Z} - \frac{\partial W_1}{\partial X}\right) \\ \frac{1}{2}\left(\frac{\partial V_1}{\partial X} - \frac{\partial U_1}{\partial Y}\right) \end{Bmatrix}, \tag{3}$$

$$\begin{Bmatrix} \chi_{XX} \\ \chi_{YY} \\ \chi_{XY} \\ \chi_{XZ} \\ \chi_{YZ} \end{Bmatrix} = \begin{Bmatrix} \frac{\partial^2 W}{\partial X \partial y} \\ -\frac{\partial^2 W}{\partial X \partial Y} \\ -\frac{1}{2}\left(\frac{\partial^2 W}{\partial X^2} - \frac{\partial^2 W}{\partial Y^2}\right) \\ -\frac{1}{4}\left(\frac{\partial^2 U}{\partial X \partial Y} - \frac{\partial^2 V}{\partial X^2}\right) \\ -\frac{1}{4}\left(\frac{\partial^2 U}{\partial Y^2} - \frac{\partial^2 V}{\partial X \partial Y}\right) \end{Bmatrix}, \tag{4}$$

A brief review on the Modified Couple Stress Theory (MCST) is given in Appendix A. According to Kirchhoff's hypothesis, the substitution of Eq. (2) into Eq. (A.2) results in the following stress components as functions of displacements:

$$\begin{Bmatrix} \sigma_{XX} \\ \sigma_{YY} \\ \sigma_{XY} \end{Bmatrix} = \frac{E}{1-\upsilon^2} \begin{bmatrix} 1 & \upsilon & 0 \\ \upsilon & 1 & 0 \\ 0 & 0 & (1-\upsilon)/2 \end{bmatrix} \left(\begin{Bmatrix} \frac{\partial U}{\partial X} + \frac{1}{2}\left(\frac{\partial W}{\partial X}\right)^2 \\ \frac{\partial V}{\partial Y} + \frac{1}{2}\left(\frac{\partial W}{\partial Y}\right)^2 \\ \frac{\partial U}{\partial Y} + \frac{\partial V}{\partial X} + \frac{\partial W}{\partial X}\frac{\partial W}{\partial Y} \end{Bmatrix} - Z \begin{Bmatrix} W_{,XX} \\ W_{,YY} \\ 2W_{,XY} \end{Bmatrix} \right) \tag{5}$$

where comma stands for the partial derivative, so the subscripts $'i = (X, Y, XX, XY, YY)'$ denote respectively $(\frac{\partial}{\partial X}, \frac{\partial}{\partial Y}, \frac{\partial^2}{\partial X^2}, \frac{\partial^2}{\partial X \partial Y}, \frac{\partial^2}{\partial Y^2})$. Inserting Eq. (4) into Eq. (A.4) leads the following relation between the deviatoric part of the couple stress and the displacements of the mid-plane.

$$\begin{Bmatrix} m_{XX} \\ m_{YY} \\ m_{XY} \\ m_{XZ} \\ m_{YZ} \end{Bmatrix} = \frac{El^2}{1+\upsilon} \begin{bmatrix} 1 & 0 & 0 & 0 & 0 \\ 0 & 1 & 0 & 0 & 0 \\ 0 & 0 & \frac{1}{2} & 0 & 0 \\ 0 & 0 & 0 & \frac{1}{4} & 0 \\ 0 & 0 & 0 & 0 & \frac{1}{4} \end{bmatrix} \begin{Bmatrix} \frac{\partial^2 W}{\partial X \partial Y} \\ -\frac{\partial^2 W}{\partial X \partial Y} \\ \frac{\partial^2 W}{\partial Y^2} - \frac{\partial^2 W}{\partial X^2} \\ \frac{\partial^2 V}{\partial X^2} - \frac{\partial^2 U}{\partial X \partial Y} \\ \frac{\partial^2 V}{\partial X \partial Y} - \frac{\partial^2 U}{\partial Y^2} \end{Bmatrix} \tag{6}$$

The governing equations of motion and associated boundary conditions for the micro-plate can be derived by using Hamilton's principle (See Appendix B). Upon substitution of Eqs. (B.11a)–(B.11c) into Eqs. (B.9a)–(B.9c), the governing equations of motion can be obtained:

$$\frac{\partial^2 U}{\partial X^2} + \frac{1}{2}(1+\upsilon)\left(\frac{\partial^2 V}{\partial X \partial Y} + \frac{\partial W}{\partial Y}\frac{\partial^2 W}{\partial X \partial Y}\right) + \frac{1}{2}(1-\upsilon)\left(\frac{\partial^2 U}{\partial Y^2} + \frac{\partial W}{\partial X}\frac{\partial^2 W}{\partial Y^2}\right)$$
$$+ \frac{\partial W}{\partial X}\frac{\partial^2 W}{\partial X^2} + \frac{l^2(1-\upsilon)}{8}\nabla^2\left(\frac{\partial^2 V}{\partial X \partial Y} - \frac{\partial^2 U}{\partial Y^2}\right) = \frac{1-\upsilon^2}{Eh} I_0 \frac{\partial^2 U}{\partial t^2}, \tag{7}$$

Please cite this article as: I. Karimipour, Y.T. Beni and A.H. Akbarzadeh, Size-dependent nonlinear forced vibration and dynamic stability of electrically actuated micro-plates, Commun Nonlinear Sci Numer Simulat, https://doi.org/10.1016/j.cnsns.2019.104856

$$\frac{\partial^2 V}{\partial Y^2}+\frac{1}{2}(1+\upsilon)\left(\frac{\partial^2 U}{\partial X\partial Y}+\frac{\partial W}{\partial X}\frac{\partial^2 W}{\partial X\partial Y}\right)+\frac{1}{2}(1-\upsilon)\left(\frac{\partial^2 V}{\partial X^2}+\frac{\partial W}{\partial Y}\frac{\partial^2 W}{\partial X^2}\right)+\frac{\partial W}{\partial Y}\frac{\partial^2 W}{\partial Y^2}+\frac{l^2(1-\upsilon)}{8}\nabla^2\left(\frac{\partial^2 U}{\partial X\partial Y}-\frac{\partial^2 V}{\partial X^2}\right)=\frac{1-\upsilon^2}{Eh}I_0\frac{\partial^2 V}{\partial t^2}, \tag{7b}$$

$$\left(\mu h l^2+\frac{Eh^3}{12(1-\upsilon^2)}\right)\nabla^4 W+I_0\frac{\partial^2 W}{\partial t^2}=I_2\frac{\partial^2}{\partial t^2}\left(\nabla^2 W\right)+\mathrm{Y}_{XX}\frac{\partial^2 W}{\partial X^2}+2\mathrm{Y}_{XY}\frac{\partial^2 W}{\partial X\partial Y}+\mathrm{Y}_{YY}\frac{\partial^2 W}{\partial Y^2}+N^r_{XX}\frac{\partial^2 W}{\partial X^2}+N^r_{YY}\frac{\partial^2 W}{\partial Y^2}+\frac{\varepsilon_0 V(t)^2}{2(g-W)^2}-\frac{Ehl^2}{8(1+\upsilon)}\left(\nabla^2\left(\frac{\partial^2 V}{\partial X\partial Y}-\frac{\partial^2 U}{\partial Y^2}\right)\frac{\partial W}{\partial X}+\nabla^2\left(\frac{\partial^2 U}{\partial X\partial Y}-\frac{\partial^2 V}{\partial X^2}\right)\frac{\partial W}{\partial Y}\right) \tag{7c}$$

Eqs. (7a)–(7c) are the non-homogeneous form of the dynamic equations of micro-plate by the combined applied voltages AC and DC. Where the operators ∇^2 and ∇^4 in two-dimensional space can be stated as:

$$\nabla^2=\left(\frac{\partial^2}{\partial X^2}+\frac{\partial^2}{\partial Y^2}\right), \tag{8}$$

$$\nabla^4=\nabla^2\nabla^2=\left(\frac{\partial^4}{\partial X^4}+2\frac{\partial^4}{\partial X^2\partial y^2}+\frac{\partial^4}{\partial Y^4}\right) \tag{9}$$

Also, the MEM plates are often slender, i.e., $b>100h$, so the in-plane oscillations in comparison to the transverse vibration are quite small and insignificant. Also, it is easy to ignore the in-plane accelerations against the transverse plate acceleration [4,65]. Furthermore, in these structures, the transverse rotational acceleration can be neglected against its transmitted acceleration [65]. So, the inertia terms $I_0\frac{\partial^2 U}{\partial t^2}$ and $I_0\frac{\partial^2 V}{\partial t^2}$ in Eq. (7a) and (b) can be neglected. Furthermore, because of the slenderness of micro-plate, the rotary inertia term $I_2\frac{\partial^2}{\partial t^2}(\nabla^2 W)$ is also insignificant in comparison to the translatory one (i.e., $I_0\frac{\partial^2 W}{\partial t^2}$) and can be ignored too [52]. It should be noted that the limitations of classical plate theory are depends on three different factors: the curvatures should be small, the in-plane plate dimensions should be large compared to the thickness and membrane strains can be neglected. So Eqs. (B.9a)–(B.9c) can be rewritten as follows:

$$\frac{\partial}{\partial X}\mathrm{Y}_{XX}+\frac{\partial}{\partial Y}\mathrm{Y}_{XY}+\frac{1}{2}\left(\frac{\partial^2}{\partial X\partial Y}\Gamma_{XZ}+\frac{\partial^2}{\partial Y^2}\Gamma_{YZ}\right)=0, \tag{10}$$

$$\frac{\partial}{\partial X}\mathrm{Y}_{XY}+\frac{\partial}{\partial Y}\mathrm{Y}_{YY}-\frac{1}{2}\left(\frac{\partial^2}{\partial X^2}\Gamma_{XZ}+\frac{\partial^2}{\partial X\partial Y}\Gamma_{YZ}\right)=0, \tag{10b}$$

$$\frac{\partial^2\Xi_{XX}}{\partial X^2}+2\frac{\partial^2\Xi_{XY}}{\partial X\partial Y}+\frac{\partial^2\Xi_{YY}}{\partial Y^2}+\mathrm{Y}_{XX}\frac{\partial^2 W}{\partial X^2}+2\mathrm{Y}_{XY}\frac{\partial^2 W}{\partial X\partial Y}+\mathrm{Y}_{YY}\frac{\partial^2 W}{\partial Y^2}+\frac{\partial\mathrm{Y}_{XX}}{\partial X}\frac{\partial W}{\partial X}+\frac{\partial\mathrm{Y}_{XY}}{\partial X}\frac{\partial W}{\partial Y}+\frac{\partial\mathrm{Y}_{XY}}{\partial Y}\frac{\partial W}{\partial X}+\frac{\partial\mathrm{Y}_{YY}}{\partial Y}\frac{\partial W}{\partial Y}+N^r_{XX}\frac{\partial^2 W}{\partial X^2}+N^r_{YY}\frac{\partial^2 W}{\partial Y^2}+\frac{\partial^2}{\partial X^2}\Gamma_{XY}-\frac{\partial^2}{\partial Y^2}\Gamma_{XY}+\frac{\partial^2}{\partial X\partial Y}\Gamma_{YY}-\frac{\partial^2}{\partial X\partial Y}\Gamma_{XX}+\frac{\varepsilon_0 V(t)^2}{2(g-W)^2}=I_0\ddot{W} \tag{10c}$$

By introducing the stress functions as follow, Eq. (10a) and (b) are automatically satisfied.

$$\mathrm{Y}_{XX}=\phi_{,YY},\ \mathrm{Y}_{YY}=\phi_{,XX},\ \mathrm{Y}_{XY}=-\phi_{,XY},\ \Gamma_{XZ}=\phi_{,Y},\ \Gamma_{YZ}=-\phi_{,X} \tag{11}$$

So, Eq. (10c) is converted as follows:

$$\frac{\partial^2}{\partial X^2}\Xi_{XX}+2\frac{\partial^2}{\partial X\partial Y}\Xi_{XY}+\frac{\partial^2}{\partial Y^2}\Xi_{YY}+\phi_{,YY}\frac{\partial^2 W}{\partial X^2}-2\phi_{,XY}\frac{\partial^2 W}{\partial X\partial Y}+\phi_{,XX}\frac{\partial^2 W}{\partial Y^2}+\frac{\partial(\phi_{,YY})}{\partial X}\frac{\partial W}{\partial X}-\frac{\partial(\phi_{,XY})}{\partial X}\frac{\partial W}{\partial Y}-\frac{\partial(\phi_{,XY})}{\partial Y}\frac{\partial W}{\partial X}+\frac{\partial(\phi_{,XX})}{\partial Y}\frac{\partial W}{\partial Y}+N^r_{XX}\frac{\partial^2 W}{\partial X^2}+N^r_{YY}\frac{\partial^2 W}{\partial Y^2}+\frac{\partial^2}{\partial X^2}\Gamma_{XY}-\frac{\partial^2}{\partial Y^2}\Gamma_{XY}+\frac{\partial^2\Gamma_{YY}}{\partial X\partial Y}-\frac{\partial^2\Gamma_{XX}}{\partial X\partial Y}+\frac{\varepsilon_0 V(t)^2}{2(g-W)^2}=I_0\ddot{W} \tag{12}$$

Please cite this article as: I. Karimipour, Y.T. Beni and A.H. Akbarzadeh, Size-dependent nonlinear forced vibration and dynamic stability of electrically actuated micro-plates, Commun Nonlinear Sci Numer Simulat, https://doi.org/10.1016/j.cnsns.2019.104856

By replacing $\Xi_i, \Gamma_i \quad i = XX, YY, XY$ from the relations (B.11a) and (B.11b), the following equation is obtained:

$$\frac{\partial^2}{\partial X^2}\left(\frac{-Eh^3}{12(1-\upsilon^2)}\frac{\partial^2 W}{\partial X^2}+\frac{-Eh^3\upsilon}{12(1-\upsilon^2)}\frac{\partial^2 W}{\partial Y^2}\right)+2\frac{\partial^2}{\partial X\partial Y}\left(\frac{-Eh^3}{12(1+\upsilon)}\frac{\partial^2 W}{\partial Y\partial X}\right)$$
$$+\frac{\partial^2}{\partial Y^2}\left(\frac{-Eh^3}{12(1-\upsilon^2)}\frac{\partial^2 W}{\partial Y^2}+\frac{-Eh^3\upsilon}{12(1-\upsilon^2)}\frac{\partial^2 W}{\partial X^2}\right)+\phi_{,YY}\frac{\partial^2}{\partial X^2}W-2\phi_{,XY}\frac{\partial^2 W}{\partial X\partial Y}$$
$$+\phi_{,XX}\frac{\partial^2}{\partial Y^2}W+\frac{\partial(\phi_{,YY})}{\partial X}\frac{\partial W}{\partial X}-\frac{\partial(\phi_{,XY})}{\partial X}\frac{\partial W}{\partial Y}-\frac{\partial(\phi_{,XY})}{\partial Y}\frac{\partial W}{\partial X}+\frac{\partial(\phi_{,XX})}{\partial Y}\frac{\partial W}{\partial Y}$$
$$+N^r_{XX}\frac{\partial^2 W}{\partial X^2}+N^r_{YY}\frac{\partial^2 W}{\partial Y^2}-\frac{1}{2}\frac{Ehl^2}{1+\upsilon}\frac{\partial^2}{\partial X^2}\left(\frac{\partial^2 W}{\partial X^2}-\frac{\partial^2 W}{\partial Y^2}\right)$$
$$+\frac{1}{2}\frac{Ehl^2}{1+\upsilon}\frac{\partial^2}{\partial Y^2}\left(\frac{\partial^2 W}{\partial X^2}-\frac{\partial^2 W}{\partial Y^2}\right)-\frac{Ehl^2}{1+\upsilon}\frac{\partial^2}{\partial X\partial Y}\left(\frac{\partial^2}{\partial X\partial Y}W\right)$$
$$-\frac{Ehl^2}{1+\upsilon}\frac{\partial^2}{\partial X\partial Y}\left(\frac{\partial^2}{\partial X\partial Y}W\right)+\frac{\varepsilon_0 V(t)^2}{2(g-W)^2}=I_0\ddot{W} \tag{13}$$

By removing U and V from Eq. (2), the compatibility equation is obtained as follows:

$$\frac{\partial^2 \varepsilon^{(0)}_{XX}}{\partial Y^2}+\frac{\partial^2 \varepsilon^{(0)}_{YY}}{\partial X^2}-\frac{\partial^2 \varepsilon^{(0)}_{XY}}{\partial X\partial Y}=\left(\frac{\partial^2 W}{\partial X\partial Y}\right)^2-\frac{\partial^2 W}{\partial X^2}\frac{\partial^2 W}{\partial Y^2} \tag{14}$$

By solving Eqs. (B.11a) and (B.11c) for $\varepsilon^0_k,\ k = XX, YY, XY$ and replacing Eq. (11), the following relations are obtained:

$$\varepsilon^{(0)}_{XX}=\frac{1}{Eh}(\phi_{,YY}-\upsilon\phi_{,XX}), \tag{15}$$

$$\varepsilon^{(0)}_{YY}=\frac{1}{Eh}(-\nu\phi_{,YY}+\phi_{,XX}), \tag{15b}$$

$$\varepsilon^{(0)}_{XY}=-2\frac{1+\upsilon}{Eh}\phi_{,XY} \tag{15c}$$

Replacing the relationships (15a) –(c) in Eq. (14) and assume that ϕ is replaced by $\phi = hF$, in which F is the Airy stress function, the following equations are obtained:

$$\nabla^4 F=E\left(W^2_{,XY}-W_{,XX}W_{,YY}\right) \tag{16}$$

By simplifying Eq. (13), Eq. (17) is obtained as follows:

$$\Lambda(W,F)\equiv h\left(F_{,YY}\frac{\partial^2}{\partial X^2}W-2F_{,XY}\frac{\partial^2}{\partial X\partial Y}W+F_{,XX}\frac{\partial^2}{\partial Y^2}W\right)+N^r_{XX}\frac{\partial^2 W}{\partial X^2}$$
$$+N^r_{YY}\frac{\partial^2 W}{\partial Y^2}+q-I_0\ddot{W}-\left(\nabla^4 W\right)D_{eq}=0 \quad \&D_{eq}=\left(\frac{1}{2}\frac{Ehl^2}{1+\upsilon}+\frac{Eh^3}{12(1-\upsilon^2)}\right),$$
$$q(X,Y)=\frac{\varepsilon_0 V(t)^2}{2(g-W(X,Y))^2} \tag{17}$$

Eqs. (16) and (17) are governing equations of micro-plate regarding W and F.

The associated out-of-plane boundary conditions for clamped micro-plate with immovable edges have the form as:

$$W=W_{,X}=0 \qquad at \qquad X=\pm\frac{a}{2}$$
$$W=W_{,Y}=0 \qquad at \qquad Y=\pm\frac{b}{2} \tag{18}$$

The in-plane conditions for clamped boundary condition are considered as (All edges immovably constrained):

$$U=F_{,XY}=0 \qquad at \qquad X=\pm\frac{a}{2}$$
$$V=F_{,XY}=0 \qquad at \qquad Y=\pm\frac{b}{2} \tag{18b}$$

Since the effect of shear deformation on the resonance frequencies of thin micro plates is not negligible, one may suspect that there are other thin-plate geometries where in-plane motion is important. So, in this condition resonant frequencies

Please cite this article as: I. Karimipour, Y.T. Beni and A.H. Akbarzadeh, Size-dependent nonlinear forced vibration and dynamic stability of electrically actuated micro-plates, Commun Nonlinear Sci Numer Simulat, https://doi.org/10.1016/j.cnsns.2019.104856

predicted by classical plate theory would be agree well with those measured by first shear deformation theory or higher plate theories. According to what is commonly stated in the literature, when in-plane motion is restricted one can assume that classical plate theory is applicable simply because the plate is thin [66].

Eqs. (16) and (17) should be solved in conjunction with boundary conditions (18a, 18b).

3. Solution procedure

Approximate methods for rectangular and circular plates with different boundary conditions were obtained by Yamaki [67]. Kung and Pao [68] used the combination of the Galerkin method and the Harmonic Balance Method (HBM) to analyze the vibration of buckled rectangular plates. Using the method of multiple scales, Hadian and Nayfeh [69] studied the response of circular plates under intermittent external stimulation. Shi and Mei [70] studied large amplitude free vibration of plates using the Reduced Order method (ROM). A large number of researchers have used the combination of finite element method and Harmonic Balance method to study the nonlinear geometric vibration of thin isotropic plates. The dynamical behavior of the plates for large-amplitude vibrations by theoretical and laboratory methods has been investigated by Benamar et al. [71]. For further study on the nonlinear behavior of plates, one can refer to nonlinear vibration and stability books of shells and plates [72], nonlinear vibrations, nonlinear analysis of plates [73], and linear and nonlinear mechanical mechanisms [30].

3.1. Static case

Because of the limitation in applying an electrical voltage to the system, the study of static behavior of micro-plate is essential to identify the maximum DC voltage and prevent the static instability of the system. For studying static behavior, a solution is assumed in the form of a generalized double Fourier series for the static case, i.e., $I_0\ddot{W}=0$ [74].

$$W=\sum_{m=1}^{\infty}\sum_{n=1}^{\infty}W_{mn}x_m(X)y_n(Y),\qquad F=\sum_{p=1}^{\infty}\sum_{q=1}^{\infty}F_{pq}x_p(X)y_q(Y) \tag{19}$$

where W_{mn} and F_{pq} are constant coefficients to be determined and x_m, x_p are beam Eigen functions given by:

$$x_m=\frac{\cosh\alpha_m X}{\cosh\alpha_m\frac{a}{2}}-\frac{\cos\alpha_m X}{\cos\alpha_m\frac{a}{2}},\qquad y_n=\frac{\cosh\beta_n Y}{\cosh\beta_n\frac{b}{2}}-\frac{\cos\beta_n Y}{\cos\beta_n\frac{b}{2}} \tag{20}$$

All the boundary conditions (18) are satisfied if the values of α_m and β_n be the roots of the transcendental equation:

$$\tanh\lambda_m+\tan\lambda_m=0 \tag{21}$$

Where

$$\lambda_m=\alpha_m\frac{a}{2}\qquad or\qquad \beta_n\frac{b}{2} \tag{22}$$

The roots of Eq. (21) are obtained simplicity. The functions $x_m(X)$ and $y_n(Y)$ satisfy the following orthogonality relations:

$$\int_{-\frac{a}{2}}^{\frac{a}{2}}x_ix_jdX=\begin{cases}0 & i\neq j\\ a & i=j\end{cases},\qquad \int_{-\frac{b}{2}}^{\frac{b}{2}}y_iy_jdY=\begin{cases}0 & i\neq j\\ b & i=j\end{cases} \tag{23}$$

The transverse load $q(X,Y)$ is expanded into a double series:

$$q(X,Y)=\sum_{m=1}^{\infty}\sum_{n=1}^{\infty}q_{mn}x_m(X)y_n(Y) \tag{24}$$

Where

$$q_{mn}=\frac{1}{ab}\int_{-\frac{a}{2}}^{\frac{a}{2}}\int_{-\frac{b}{2}}^{\frac{b}{2}}q(X,Y)x_m(X)\;\;y_n(Y)\;dXdY \tag{25}$$

Substituting Eqs. (19) and (24) into Eqs. (17) and (16) leads to:

$$\begin{aligned}&\sum_{m=1}^{\infty}\sum_{n=1}^{\infty}W_{mn}\left((\alpha_m^4+\beta_n^4)x_my_n+2x''_my''_n\right)\;\;=\frac{1}{D_{eq}}\\&\left(\sum_{m=1}^{\infty}\sum_{n=1}^{\infty}q_{mn}x_my_n+\;h\sum_{p=1}^{\infty}\sum_{q=1}^{\infty}\sum_{r=1}^{\infty}\sum_{s=1}^{\infty}W_{pq}F_{rs}\left(x_rx''_py_qy''_s+x_px''_ry_sy''_q-2x'_px'_ry'_qy'_s\right)\right.\\&\left.+N_{XX}^r\sum_{m=1}^{\infty}\sum_{n=1}^{\infty}W_{mn}\alpha_m^2x_my_n+N_{YY}^r\sum_{m=1}^{\infty}\sum_{n=1}^{\infty}W_{mn}\beta_n^2x_my_n\right)\end{aligned} \tag{26}$$

Please cite this article as: I. Karimipour, Y.T. Beni and A.H. Akbarzadeh, Size-dependent nonlinear forced vibration and dynamic stability of electrically actuated micro-plates, Commun Nonlinear Sci Numer Simulat, https://doi.org/10.1016/j.cnsns.2019.104856

$$\sum_{p=1}^{\infty}\sum_{q=1}^{\infty}F_{pq}\left((\alpha_p^4+\beta_q^4)x_p y_q+2x''_p y''_q\right)$$
$$=E\sum_{m=1}^{\infty}\sum_{n=1}^{\infty}\sum_{r=1}^{\infty}\sum_{s=1}^{\infty}W_{mn}W_{rs}\left(x'_m x'_r y'_n y'_s-x_r x''_m y_n y''_s\right) \tag{27}$$

in which primes denote differential with respect to the corresponding coordinates. Multiplying each of Eqs. (26) and (27) by $x_i(X)\times y_j(Y)$, integrating with respect to X and Y over their respective intervals, and using Eqs. (22) and (23) leads to a system of nonlinear algebraic equations.

$$W_{ij}\left(\frac{b^2}{a^2}\lambda_i^4+\frac{a^2}{b^2}\lambda_j^4\right)+2\sum_{m=1}^{\infty}\sum_{n=1}^{\infty}W_{mn}\lambda_m^2\lambda_n^2K_1^{im}K_1^{jn}=\frac{a^2b^2q_{ij}}{16D_{eq}}+\frac{h}{D_{eq}}$$
$$\times\sum_{p=1}^{\infty}\sum_{q=1}^{\infty}\sum_{r=1}^{\infty}\sum_{s=1}^{\infty}W_{pq}F_{rs}.\left(\lambda_p^2\lambda_s^2K_2^{irp}L_2^{jqs}+\lambda_q^2\lambda_r^2K_2^{ipr}L_2^{jsq}-2\lambda_p\lambda_q\lambda_r\lambda_sK_3^{ipr}L_3^{jqs}\right),$$
$$i,j=1,2,3,\ldots \tag{28}$$

$$F_{ij}\left(\frac{b^2}{a^2}\lambda_i^4+\frac{a^2}{b^2}\lambda_j^4\right)+2\sum_{p=1}^{\infty}\sum_{q=1}^{\infty}F_{pq}\lambda_p^2\lambda_q^2K_1^{ip}K_1^{jq}$$
$$=E\sum_{m=1}^{\infty}\sum_{n=1}^{\infty}\sum_{r=1}^{\infty}\sum_{s=1}^{\infty}W_{mn}W_{rs}.(\lambda_m\lambda_n\lambda_r\lambda_sK_3^{imr}L_3^{jns}-\lambda_m^2\lambda_s^2K_2^{irm}L_2^{jns}),\quad i,j=1,2,3,\ldots \tag{29}$$

where

$$K_1^{im}=\frac{1}{a\alpha_m^2}\int_{-\frac{a}{2}}^{\frac{a}{2}}x_i x''_m dX\ ,\ L_1^{jn}=\frac{1}{b\beta_n^2}\int_{-\frac{b}{2}}^{\frac{b}{2}}y_j y''_n dY, K_2^{irp}=\frac{1}{a\alpha_p^2}\int_{-\frac{a}{2}}^{\frac{a}{2}}x_i x_r x''_p dX,$$
$$L_2^{jqs}=\frac{1}{b\beta_s^2}\int_{-\frac{b}{2}}^{\frac{b}{2}}y_j y_q y''_s dY,\ K_3^{ipr}=\frac{1}{a\alpha_p\alpha_r}\int_{-\frac{a}{2}}^{\frac{a}{2}}x_i x'_p x'_r dX,\ L_3^{jqs}=\frac{1}{b\beta_q\beta_s}\int_{-\frac{b}{2}}^{\frac{b}{2}}y_j y'_q y'_s dY \tag{30}$$

Let $q(X,Y)$ be load P uniformly distributed over a portion of the plate surface. The load coefficients introduced in Eq. (25) become:

$$q_{mn}=\frac{P}{\alpha\beta\lambda_m\lambda_n}(\sinh\lambda_m-\sin\lambda_m)\ (\sinh\lambda_n-\sin\lambda_n) \tag{31}$$

By substituting Eq. (31) into Eq. (28), the deflection vector and stress resultants can be calculated. With these values of q_{mn}, the geometrically nonlinear behavior of a rectangular micro-plate under a uniformly distributed load (P) can be investigated by the previous series solution. Similarly, the solution can be applied to other types of transverse loading.

3.1.1. Galerkin's method for clamped micro-plate

The large deflection of a rectangular clamped micro-plate under distributed load $q(X,Y)$ is reconsidered by making use of the one-term approximation of the Galerkin method [75]. The equilibrium Eq. (17) and compatibility relation (16) and boundary conditions (38) remain unchanged. The transverse deflection is assumed to be of the form Yeh and Liu [76]

$$W=gW_m\cos^2\left(\frac{\pi X}{a}\right)\cos^2\left(\frac{\pi Y}{b}\right) \tag{32}$$

in which W_m, is the non-dimensional maximum deflection at the plate center given by $W_{0/g}$, and W_0 denotes the central deflection. This approximated deflection obviously satisfies the geometrical boundary conditions in Eq. (18). Upon substitution Eq. (16) may be expressed as:

$$\nabla^4F=-\frac{\pi^4Eg^2W_m^2}{a^2b^2}\sum_{p=0}^{\infty}\sum_{q=0}^{\infty}a_{pq}R_p(X)S_q(Y) \tag{33}$$

Where

$$R_p(X)=\cos\frac{2p\pi X}{a}\ ,\quad S_q(Y)=\cos\frac{2q\pi Y}{b},\ a_{01}=a_{10}=a_{02}=a_{20}=a_{12}=$$
$$a_{21}=\frac{1}{2}\ ,\ a_{11}=1\ \ and\ all\ \ other\ \ a_{pq}=0 \tag{34}$$

Please cite this article as: I. Karimipour, Y.T. Beni and A.H. Akbarzadeh, Size-dependent nonlinear forced vibration and dynamic stability of electrically actuated micro-plates, Commun Nonlinear Sci Numer Simulat, https://doi.org/10.1016/j.cnsns.2019.104856

The general solution of Eq. (33) is the sum of the complementary function F_c and a particular integral F_p, i.e., $F = F_c + F_p$. A particular solution of Eq. (33) may be expressed as:

$$F_p = Eg^2W_m^2\sum_{p=0}^{\infty}\sum_{q=0}^{\infty} b_{pq}R_p(X)S_q(Y)\ \&b_{pq} = -\frac{\psi^2 a_{pq}}{16(p^2+\psi^2q^2)^2}\ ,\ \psi = \frac{a}{b} \tag{35}$$

It is easily seen that F_p given by expression (35) is an even function of X and Y with the vanishing shear stresses along the boundaries. With the same properties, the complementary function may be expressed in the form:

$$\begin{aligned} F_c = {} & \frac{W_m^2}{2}(C_1X^2 + C_2Y^2) + Eg^2W_m^2\sum_{n=1}^{\infty}\left\{\frac{A_n}{n^2[\sinh(n\pi/\psi)\cosh(n\pi/\psi)+n\pi/\psi]}\right. \\ & \left[\left(\sinh\frac{n\pi}{\psi}+\frac{n\pi}{\psi}\cosh\frac{n\pi}{\psi}\right)\cosh\frac{2n\pi}{a}Y - \frac{2n\pi}{a}Y\sinh\frac{n\pi}{\psi}\sinh\frac{2n\pi}{a}Y\right]\cos\frac{2n\pi X}{a} \\ & + \frac{B_n}{n^2\psi^2[\sinh n\pi\psi\cosh n\pi\psi + n\pi\psi]}[(\sinh n\pi\psi + n\pi\psi\cosh n\pi\psi)\cosh\frac{2n\pi X}{b} \\ & \left. -\frac{2n\pi}{b}X\sinh n\pi\psi\sinh\frac{2n\pi}{b}X\right]\cos\frac{2n\pi}{b}Y\Bigg\} \end{aligned} \tag{36}$$

In which C_1, C_2, A_n, and B_n, are arbitrary constants. (See Appendix C, for more information). For convenience, the complementary function F_c is also represented by a double cosine series.

$$F_c = Eg^2W_m^2\sum_{p=0}^{\infty}\sum_{q=0}^{\infty} c_{pq}R_p(X)S_q(Y) \tag{37}$$

The Fourier coefficients c_{mn} in the series are given by:

$$\begin{aligned} c_{mn} = {} & \frac{4\psi}{\pi(m^2+\psi^2n^2)^2} \\ & \times\left(\frac{m(-1)^n\varsigma_n\sinh^2(m\pi/\psi)A_m}{(m\pi/\psi)+\sinh(m\pi/\psi)\cosh(m\pi/\psi)} + \frac{n(-1)^m\varsigma_m\sinh^2 n\pi\psi B_n}{n\pi\psi+\sinh n\pi\psi\cosh n\pi\psi}\right) \\ & m,n = 0,1,2,\ldots \end{aligned} \tag{38}$$

where

$$\varsigma_0 = \frac{1}{2}\ ,\ \ \varsigma_1 = \varsigma_2 = \cdots = 1 \tag{39}$$

By substitution ($F = F_c + F_p$) yields:

$$F = Eg^2W_m^2\sum_{p=0}^{\infty}\sum_{q=0}^{\infty}(b_{pq}+c_{pq})R_p(X)S_q(Y) \tag{40}$$

Function (32) for W and Function (36) for F satisfy all the boundary conditions (18) as well as the compatibility condition (16). With these expressions, however, the equilibrium Eq. (16) generally cannot be precisely satisfied. Instead of satisfaction of this equation, we apply the Galerkin method to minimize the error function which is obtained by inserting Eqs. (32) and (40) into (16), i.e.,

$$\iint_A \Lambda(W,F)W\ dX\ dY = 0 \tag{41}$$

3.2. Vibrational of micro-plate due to the harmonic electrical force

The in-plane displacements U and V are related to the stress function (F) by the following equation:

$$U = \int_0^X\left(\frac{(F_{,YY}-\upsilon F_{,XX})}{E} - \frac{1}{2}(W_{,X})^2\right)dX\&V = \int_0^Y\left(\frac{(F_{,XX}-\upsilon F_{,YY})}{E} - \frac{1}{2}(W_{,Y})^2\right)dY \tag{42}$$

A one-term approximate solution of the governing Eqs. (16) and (17) satisfying the prescribed boundary conditions in each case which formulated by application of the Galerkin method. The conditions (18a) are satisfied by assuming the deflection function as [77]:

$$W = gR(t)\cos^2\left(\frac{\pi X}{a}\right)\cos^2\left(\frac{\pi Y}{b}\right) \tag{43}$$

in which $R(t)$ is a function of time (t) with its maximum value being:

$$R_{\max}(t) = \frac{W_m}{g} \tag{44}$$

Please cite this article as: I. Karimipour, Y.T. Beni and A.H. Akbarzadeh, Size-dependent nonlinear forced vibration and dynamic stability of electrically actuated micro-plates, Commun Nonlinear Sci Numer Simulat, https://doi.org/10.1016/j.cnsns.2019.104856

In this expression W_m, is the maximum deflection of the plate. Substituting expressions (43) into the compatibility Eq. (16) yields:

$$\nabla^4 F = \frac{\pi^4 E g^2 R^2}{a^2 b^2} \sum_{p=0}^{\infty} \sum_{q=0}^{\infty} a_{pq} \cos \frac{2p\pi X}{a} \cos \frac{2q\pi Y}{b} \tag{45}$$

in which a_{pq} are known Fourier coefficients. The general solution of Eq. (45) is $F = F_c + F_p$, where F_c is the complementary function and F_p is a particular solution which may be expressed as:

$$F_p = E g^2 R^2 \sum_{p=0}^{\infty} \sum_{q=0}^{\infty} b_{pq} \cos \frac{2p\pi X}{a} \cos \frac{2q\pi Y}{b} \quad , b_{pq} = \frac{\psi^2 a_{pq}}{16(p^2 + \psi^2 q^2)^2} \tag{46}$$

After some manipulation the nonzero coefficients b_{pq} are obtained:

$$b_{01} = -\frac{1}{32\psi^2}, \quad b_{10} = -\frac{\psi^2}{32}, \quad b_{11} = -\frac{\psi^2}{16(1+\psi^2)^2}, \quad b_{02} = -\frac{1}{512\psi^2},$$
$$b_{20} = -\frac{\psi^2}{512}, \quad b_{12} = -\frac{\psi^2}{32(1+4\psi^2)^2}, \quad b_{21} = -\frac{\psi^2}{32(4+\psi^2)^2} \tag{47}$$

It is observed that F_p, is an even function in X and Y satisfying the condition for zero shear stress along the edges of the plate. The constants C_1, C_2, A_n and B_n in Eq. (36) are to be determined by the in-plane boundary conditions. Inserting the expressions W and F in conditions (18b), by use of Eq. (42), for an immovable micro-plate, these constants obtained as:

$$C_1 = \frac{3}{32} \frac{\pi^2 E g^2 (\psi^2 + \upsilon)}{a^2 (1 - \upsilon^2)}, \quad C_2 = \frac{3}{32} \frac{\pi^2 E g^2 (\upsilon\psi^2 + 1)}{a^2 (1 - \upsilon^2)}, A_n = B_n = 0 \tag{48}$$

Now the function F can be written in the general form:

$$F = \frac{R^2}{2}(C_1 X^2 + C_2 Y^2) + E g^2 R^2 \sum_{p=0}^{\infty} \sum_{q=0}^{\infty} b_{pq} \cos \frac{2p\pi X}{a} \cos \frac{2q\pi Y}{b} \tag{49}$$

Finally, the following equation is obtained for F:

$$\begin{aligned} F = {} & \frac{R^2}{2} \left(\frac{3}{32} \frac{\pi^2 E g^2 (\psi^2 + \upsilon)}{a^2 (1 - \upsilon^2)} X^2 + \frac{3}{32} \frac{\pi^2 E g^2 (\upsilon\psi^2 + 1)}{a^2 (1 - \upsilon^2)} Y^2 \right) - E g^2 R^2 \\ & \times \left(\frac{1}{32\psi^2} \cos \frac{2\pi Y}{b} + \frac{\psi^2}{32} \cos \frac{2\pi X}{a} + \frac{\psi^2}{16(1+\psi^2)^2} \cos \frac{2\pi X}{a} \cos \frac{2\pi Y}{b} \right. \\ & + \frac{1}{512\psi^2} \cos \frac{4\pi Y}{b} + \frac{\psi^2}{512} \cos \frac{4\pi X}{a} + \frac{\psi^2}{32(1+4\psi^2)^2} \cos \frac{2\pi X}{a} \cos \frac{4\pi Y}{b} \\ & \left. + \frac{\psi^2}{32(4+\psi^2)^2} \cos \frac{4\pi X}{a} \cos \frac{2\pi Y}{b} \right) \end{aligned} \tag{50}$$

3.3. Non-dimensionalization of the governing equations

It is an excellent practice to non-dimensionalize the governing equations before treating them with perturbation methods to simplify and avoid calculation errors. To this end, the non-dimensionalization parameters such as characteristic length, time and other non-dimensional variables are as follow:

$$x = \frac{X}{a}, \quad y = \frac{Y}{b}, \quad w = \frac{W}{g}, \psi = \frac{a}{b}, \ \xi = 6(1-\upsilon)\left(\frac{l}{h}\right)^2, \ f = \frac{F}{E g^2}, \kappa = \frac{g}{h},$$
$$N_{i=x,y} = \frac{12a^2(1-\upsilon^2)N_i^r}{Eh^3}, \hat{t} = \frac{t}{a^2}\sqrt{\frac{Eh^3}{12(1-\upsilon^2)\rho h}}, \quad \beta = \frac{6(1-\upsilon^2)\varepsilon_0 a^4}{Eh^3 g^3} \tag{51}$$

Upon substitution of the dimensionless quantities given in Eq. (51) into Eqs. (16), (17) and (50) moreover, multiplication both side Eqs. (16) and (17) by $\frac{a^4}{g}\frac{12(1-\upsilon^2)}{Eh^3}$ and Eq. (50) by $\frac{a^4}{Eg^2}$ the following equations will be gained:

$$12\psi^2\kappa^2(1-\upsilon^2)\left(f_{,yy}\frac{\partial^2}{\partial x^2}w - 2f_{,xy}\frac{\partial^2}{\partial x \partial y}w + f_{,xx}\frac{\partial^2}{\partial y^2}w\right) + N_x\frac{\partial^2 w}{\partial x^2}$$

Please cite this article as: I. Karimipour, Y.T. Beni and A.H. Akbarzadeh, Size-dependent nonlinear forced vibration and dynamic stability of electrically actuated micro-plates, Commun Nonlinear Sci Numer Simulat, https://doi.org/10.1016/j.cnsns.2019.104856

$$+N_y\psi^2\frac{\partial^2 w}{\partial y^2}+\frac{\beta V(t)^2}{(1-w)^2}-\frac{\partial^2 w}{\partial t^2}=\frac{\partial^4 w}{\partial x^4}+2\psi^2\frac{\partial^4 w}{\partial x^2\partial y^2}+\psi^4\frac{\partial^4 w}{\partial y^4}$$
$$+\xi\left(\frac{\partial^4 w}{\partial x^4}+2\psi^2\frac{\partial^4 w}{\partial x^2\partial y^2}+\psi^4\frac{\partial^4 w}{\partial y^4}\right), \tag{52}$$

$$\frac{\partial^4 f}{\partial x^4}+2\psi^2\frac{\partial^4 f}{\partial x^2\partial y^2}+\psi^4\frac{\partial^4 f}{\partial y^4}+\psi^2\left(\frac{\partial^2 w}{\partial x^2}\frac{\partial^2 w}{\partial y^2}-\left(\frac{\partial^2 w}{\partial x\partial y}\right)^2\right)=0, \tag{53}$$

$$f=\frac{R^2\pi^2}{2}\left(\frac{3}{32}\frac{\left(\psi^2+\upsilon\right)}{\left(1-\upsilon^2\right)}x^2+\frac{3}{32}\frac{\left(\upsilon\psi^2+1\right)}{\left(1-\upsilon^2\right)}y^2\right)-R^2$$
$$\times\left(\frac{1}{32\psi^2}\cos 2\pi y+\frac{\psi^2}{32}\cos 2\pi x+\frac{\psi^2}{16\left(1+\psi^2\right)^2}\cos 2\pi x\cos 2\pi y\right.$$
$$+\frac{1}{512\psi^2}\cos 4\pi y+\frac{\psi^2}{512}\cos 4\pi x+\frac{\psi^2}{32\left(1+4\psi^2\right)^2}\cos 2\pi x\cos 4\pi y$$
$$\left.+\frac{\psi^2}{32\left(4+\psi^2\right)^2}\cos 4\pi x\cos 2\pi y\right) \tag{54}$$

Eqs. (52) and (53) are equations of motion for the rectangular micro-plates under electric force in terms of w and f. In other words, Eq. (52) states the movement of the micro-plate in the Z direction and Eq. (53) is the plate compatibility equation. It can be understood that the length of the plate has a substantial effect on the static and dynamic components of the electrical force β (see Eq. (51)).

3.3.1. Non-dimensionalization of the boundary conditions

The associated in-plane and out-plane dimensionless boundary conditions for micro-plate with immovable edges have the form as [52, 54]

$$\begin{aligned}
\delta u&=0 \quad at\ x=-\frac{1}{2},\frac{1}{2}\ \&\ y=-\frac{1}{2},\frac{1}{2}\\
\frac{\partial\delta u}{\partial x}&=0 \quad at\ y=-\frac{1}{2},\frac{1}{2}\\
\frac{\partial\delta u}{\partial y}&=0 \quad at\ x=-\frac{1}{2},\frac{1}{2}\ \&\ y=-\frac{1}{2},\frac{1}{2}\\
\delta v&=0 \quad at\ x=-\frac{1}{2},\frac{1}{2}\ \&\ y=-\frac{1}{2},\frac{1}{2}\\
\frac{\partial\delta v}{\partial x}&=0 \quad at\ x=-\frac{1}{2},\frac{1}{2}\ \&\ y=-\frac{1}{2},\frac{1}{2}\\
\frac{\partial\delta v}{\partial y}&=0 \quad at\ x=-\frac{1}{2},\frac{1}{2}\\
\delta w&=0 \quad at\ x=-\frac{1}{2},\frac{1}{2}\ \&\ y=-\frac{1}{2},\frac{1}{2}\\
\frac{\partial\delta w}{\partial x}&=0 \quad at\ x=-\frac{1}{2},\frac{1}{2}\ \&\ y=-\frac{1}{2},\frac{1}{2}\\
\frac{\partial\delta w}{\partial y}&=0 \quad at\ x=-\frac{1}{2},\frac{1}{2}\ \&\ y=-\frac{1}{2},\frac{1}{2}
\end{aligned} \tag{55}$$

4. Obtaining a set of ordinary differential equation

The large static deflection of the plate can be treated as a special case of the nonlinear plate vibration. In the discretization methods, one postulates the solution in the form $w(x,y,t)=\sum_{m=1}^{M}\phi_m(x,y)R_m(t)$, where M is a finite integer and ϕ_m are the generalized coordinates [62]. By replacing $w=R(t)\cos^2(\pi x)\cos^2(\pi y)$ and f from Eq. (54), into Eq. (52), multiplying the resulting equation in $\cos^2(\pi x)\cos^2(\pi y)$ and integrating from $(x,y)=(-\frac{1}{2},-\frac{1}{2})$ to $(x,y)=(\frac{1}{2},\frac{1}{2})$, the following nonlinear ordinary differential equation is obtained:

$$\ddot{R}(t)+A_1R(t)\ddot{R}(t)+A_2R(t)^2\ddot{R}(t)+A_3R(t)+A_4R(t)^2+A_5R(t)^3+A_6R(t)^4$$

Please cite this article as: I. Karimipour, Y.T. Beni and A.H. Akbarzadeh, Size-dependent nonlinear forced vibration and dynamic stability of electrically actuated micro-plates, Commun Nonlinear Sci Numer Simulat, https://doi.org/10.1016/j.cnsns.2019.104856

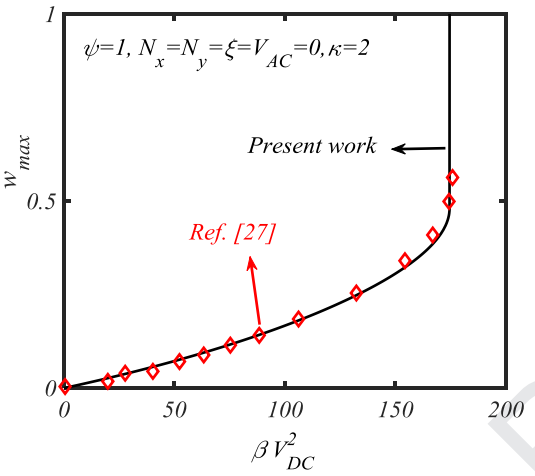

Fig. 2. Comparison between the static deflection obtained by the current method for a micro-plate.

$$+A_7R(t)^5+A_8=0 \tag{56}$$

The coefficients $A_i,\ \ i=1,2,\ldots,8$ are presented in Appendix D.

5. Result and discussion

The results presented in the next sections have been obtained for clamped micro-plates without in-plate motion and with the following coefficients $N_x=N_y=1,\ \upsilon=0.33$, wherever these coefficients have not been specified.

5.1. Validation

To measure the accuracy of the model proposed in this research, the following results are validated with the information contained in the previously published article. Fig. 2 shows a comparison between the static deflection obtained by the current method and those obtained by Zhao using a reduced order model based on analytically obtained basis functions [29]. As it is evident, there is a good agreement.

5.2. Time response and phase portrait

According to the Eq. (56) and by using a change of variables, i.e., $R(t)=y1,\ \dot{R}(t)=y2$, the following equations are obtained as:

$$\dot{y}_2=\frac{1}{\left(1+A_1y_1+A_2{y_1}^2\right)}\Big(-\left(A_3y_1+A_4{y_1}^2+A_5{y_1}^3+A_6{y_1}^4+A_7{y_1}^5\right)+\frac{16\beta}{9}\left({V^2}_{DC}+2V_{DC}V_{AC}\cos(\omega_1t)+\frac{{V^2}_{AC}}{2}(1+\cos(\omega_2t))\right)\Big),$$
$$\dot{y}_1=y_2,\qquad \Omega=\omega_1,\qquad 2\Omega=\omega_2 \tag{57}$$

One may solve the above equations using the Runge-Kutta method to obtain a time response that is shown in Fig. 3. This response is periodic (repeats with a certain period T) because the ratio between two frequencies is a rational number $\omega_2=2\omega_1$. If one plot the phase portrait by sampling at a time interval, it will yield a single point as shown in Fig. 3(c). It may be noted that the actual phase portrait is shown in Fig. 3(b). The Poincare' section of the periodic response is shown in Fig. 3(c). So, in this way, one can determine the Poincare' section by sampling the time response with the minimum period. It is the method used to reduce the dimension of the system by one. Let us take another case. Here, let excited voltage, i.e., $V(t)=(V_{DC}+{V^1}_{AC}\cos(\omega_1t)+{V^2}_{AC}\cos(\omega_2t))$ with two forcing terms having incommensurable frequencies. In this case, the ratio $\omega_2=2\sqrt{2}\omega_1$ is an irrational number so, the response will be quasi-periodic. The time response is shown in Fig. 4(a). Here the system has more one period. By taking the sampling time as T (which is the minimum period), one may plot the phase portrait as shown in Fig. 4(b). Hence, for the quasi-periodic response, the Poincare' section is not a discrete point) Fig. 4(c)). It may be noted that in the case of incommensurable frequencies, one obtains multiple loops in the phase portraits and discrete points in the Poincare section.

Please cite this article as: I. Karimipour, Y.T. Beni and A.H. Akbarzadeh, Size-dependent nonlinear forced vibration and dynamic stability of electrically actuated micro-plates, Commun Nonlinear Sci Numer Simulat, https://doi.org/10.1016/j.cnsns.2019.104856

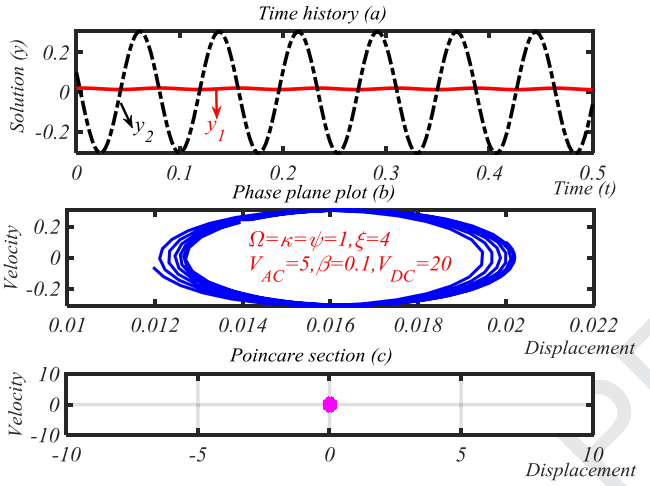

Fig. 3. Time Response, Phase portrait, and Poincare' section, $\beta = 0.1,\ \Omega = \psi = \kappa = 1,\ V_{AC} = 5, V_{DC} = 20, \xi = 4$..

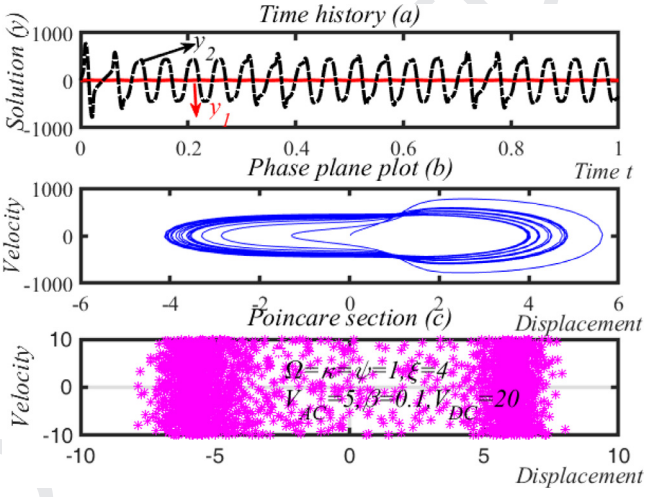

Fig. 4. Time Response, Phase portrait, and Poincare' section, $\beta = 0.1,\ V_{AC}^1 = V_{DC} = 100, \psi = \kappa = \xi = 1, V_{AC}^2 = 200, \omega_2 = 12\sqrt{2}, \omega_1 = 6$..

5.3. Static case

By solving Eq. (56) moreover, neglecting time derivatives, i.e., $(\ddot{R}(t) = 0)$, one can plot maximum static deflection of the micro-plate at $w_{\max}(x, y) = w(0, 0)$ under electrostatic load.

Fig. 5a shows the variation of the maximum deflection of the micro-plate with respect to the electrostatic voltage for different values of κ. It can be seen that in the case $\kappa = 1$, $\xi = 0.2$ the pull-in voltage is equal to $V_{DC}|_{Pull-in} = 2.5808$. In this point $\frac{\partial w_{\max}}{\partial V_{DC}}|_{V_{DC}(Pull-in)} = \infty$. In other words, in the pull-in phenomenon, for a small change in voltage, there is a significant jump in the displacement response. After pull-in phenomena, the system enters the unstable state. With increasing electrostatic force, the maximum deflection increases. This behavior is linear for small amounts of electrostatic force. By increasing the electrostatic force, this trend tends to highly nonlinear behavior. Also, by an increasing amount of κ, the pull-in voltage and maximum deflection will be increased. As seen in this figure, by increasing κ, the stiffness of the micro-plate increases, because, for a specific DC voltage, the maximum deflection of the micro-plate decrease.

Fig. 5b shows the variation of the maximum deflection of the micro-plate with respect to the electrostatic voltage for different values of ψ. As can be seen, with increasing ψ, the critical pull-in voltage, increases. As a general result, it can be said that with increasing ψ, the stiffness of the micro-plate increases.

5.3.1. A semi-analytical solution for the transient response of micro-plate

The purpose of this section is to obtain a semi-analytical relationship for the static deflection of micro-plate under electrostatic load by the method of multiple scales. The semi-analytical relationship provides the possibility for analysis of the effects of different parameters analytically. Though the method of multiple scales is a solving method for obtaining the

Please cite this article as: I. Karimipour, Y.T. Beni and A.H. Akbarzadeh, Size-dependent nonlinear forced vibration and dynamic stability of electrically actuated micro-plates, Commun Nonlinear Sci Numer Simulat, https://doi.org/10.1016/j.cnsns.2019.104856

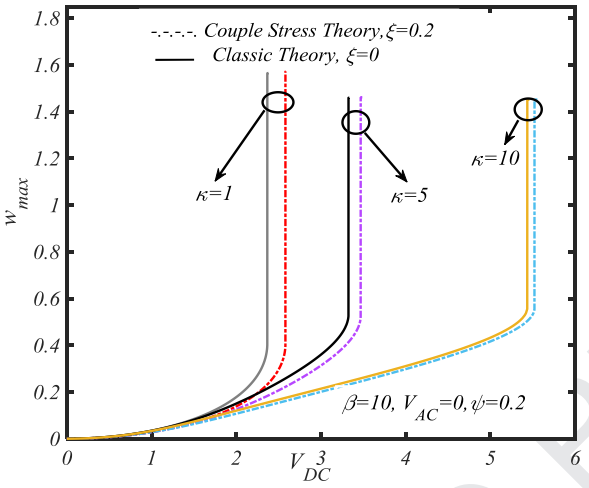

Fig. 5a. Static maximum deflection obtained for a micro-plate for different values of κ.

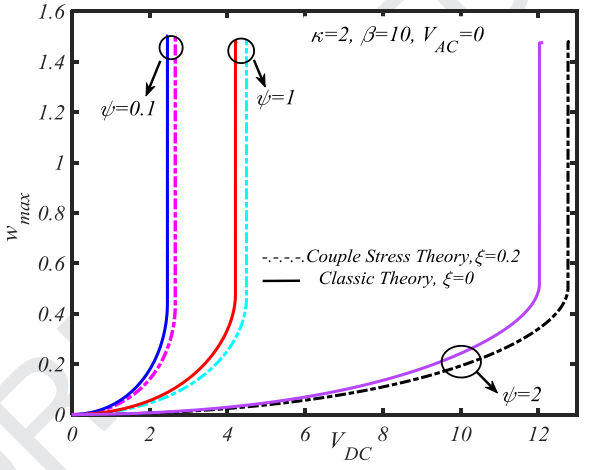

Fig. 5b. Variation of the maximum deflection of the micro-plate with respect to the electrostatic voltage for different values of ψ.

dynamic response of vibrating systems, here it is used to get the static response of the system. Approximate solution of Eq. (56) as a second-order expansion in terms of the positive and small parameter ε is as follows:

$$R(\tau_0, \tau_1, \tau_2, \varepsilon) = R_0(\tau_0, \tau_1, \tau_2) + \varepsilon R_1(\tau_0, \tau_1, \tau_2) + \varepsilon^2 R_2(\tau_0, \tau_1, \tau_2) \tag{58}$$

Where in the above equation R_0, R_1 *and* R_2 are three unknown functions. To obtain a second-order uniform expansion by using the method of multiple scales, we need the three-time scales τ_0, τ_1, and τ_2 in which are as follow:

$$\tau_0 = t, \tau_1 = \varepsilon t, \tau_2 = \varepsilon^2 t \tag{59}$$

In terms of the time scales τ_i, $i = 0, 1, 2$, the time derivatives become:

$$\frac{d}{dt} = D_0 + \varepsilon D_1 + \varepsilon^2 D_2 \& \frac{d^2}{dt^2} = D_0^2 + 2\varepsilon D_0 D_1 + 2\varepsilon^2 D_0 D_2 + \varepsilon^2 D_1^2 \tag{60}$$

in which:

$$D_0 = \frac{d}{d\tau_0}, D_1 = \frac{d}{d\tau_1}, D_2 = \frac{d}{d\tau_2} \tag{61}$$

Using the timescales, τ_i, $i = 0, 1, 2$ we transform Eq. (56) from an ordinary-differential equation into a partial differential equation:

$$\ddot{R}(t) + A_3 R(t) + \varepsilon^2 \left(A_1 R(t) \ddot{R}(t) + A_2 R(t)^2 \ddot{R}(t) + A_4 R(t)^2 + A_5 R(t)^3 + A_6 R(t)^4 + A_7 R(t)^5 \right) + A_8 = 0 \tag{62}$$

Please cite this article as: I. Karimipour, Y.T. Beni and A.H. Akbarzadeh, Size-dependent nonlinear forced vibration and dynamic stability of electrically actuated micro-plates, Commun Nonlinear Sci Numer Simulat, https://doi.org/10.1016/j.cnsns.2019.104856

Equating coefficients of like powers of $\varepsilon^0, \varepsilon^1, \varepsilon^2$ in Eq. (62):

$$O(\varepsilon^0): D_0^2 R_0 + A_3 R_0 = -A_8 \tag{63}$$

$$O(\varepsilon^1): D_0^2 R_1 + A_3 R_1 = -2D_0 D_1 R_0 \tag{63b}$$

$$O(\varepsilon^2): D_0^2 R_2 + A_3 R_2 = -2D_0 D_1 R_1 - 2D_0 D_2 R_0 - D_1^2 R_0 - A_1 R_0 D_0^2 R_0 - A_2 R_0^2 D_0^2 R_0 - A_4 R_0^2 - A_5 R_0^3 - A_6 R_0^4 - A_7 R_0^5 \tag{64c}$$

The general solution for the Eq. (63) is as follows:

$$R_0 = -\frac{A_8}{A_3} + A(\tau_1, \tau_2) e^{i\sqrt{A_3}\tau_0} + \bar{A}(\tau_1, \tau_2) e^{-i\sqrt{A_3}\tau_0} \tag{64}$$

where $A(\tau_1, \tau_2), \bar{A}(\tau_1, \tau_2)$ are the Complex Conjugate functions. By replacing Eq. (64) in (63) following equation is obtained:

$$D_0^2 R_1 + A_3 R_1 = -2i\sqrt{A_3} D_1 A(\tau_1, \tau_2) e^{i\sqrt{A_3}\tau_0} + 2i\sqrt{A_3} D_1 \bar{A}(\tau_1, \tau_2) e^{-i\sqrt{A_3}\tau_0} \tag{65}$$

Clearly, Eq. (65), breaks down because it contains secular terms and small-divisor terms. Due to R_1 be periodic, we need to eliminate the secular and small-divisor terms. Therefore, we set the coefficient $e^{\pm i\sqrt{A_3}\tau_0}$ equal to zero ($D_1 A(\tau_1, \tau_2) = D_1 \bar{A}(\tau_1, \tau_2) = 0$). This result means that $A(\tau_1, \tau_2)\&\bar{A}(\tau_1, \tau_2)$ are only functions of τ_2. Solving Eq. (65) gives Eq. (66) as follows:

$$R_1 = B(\tau_1, \tau_2) e^{i\sqrt{A_3}\tau_0} + \bar{B}(\tau_1, \tau_2) e^{i\sqrt{A_3}\tau_0} \tag{66}$$

Where $B(\tau_1, \tau_2), \bar{B}(\tau_1, \tau_2)$ are Complex Conjugate. By replacing the Eqs. (64) and (66) into Eq. (63);

$$D_0^2 R_2 = CC + O.H.T + e^{i\omega_0 t} \times \left(-2i\sqrt{A_3} D_1 B - 2i\sqrt{A_3} D_2 A - 3A_5 A^2 \bar{A} - A_1 A_8 A V_p^2 + \frac{A_2 A_8^2 A}{A_3} + 3A_2 A_3 A^2 \bar{A} + \frac{2A_4 A_8 A}{A_3} - \frac{3A_5 A_8^2 A}{A_3^2} - \frac{5A_7 A_8^4 A}{A_3^4} - \frac{30A_7 A_8^2 A^2 \bar{A}}{A_3^2} + \frac{4A_6 A_8^3 A}{A_3^3} + \frac{12A_6 A_8 A^2 \bar{A}}{A_3} - 10A_7 A^3 \bar{A}^2 \right) \tag{67}$$

where $CC\&O.H.T$ are conjugate and other harmonic terms that are neglected in the further calculations. The elimination of the secular expressions in the above equation requires that the right side of the Eq. (67) be equal to zero except for the O.H.T terms. It follows that B is a function of τ_2.

$$-2i\sqrt{A_3} D_2 A - 3A_5 A^2 \bar{A} - A_1 A_8 A + \frac{A_2 A_8^2 A}{A_3} + 3A_2 A_3 A^2 \bar{A} + \frac{2A_4 A_8 A}{A_3} - \frac{3A_5 A_8^2 A}{A_3^2} - \frac{5A_7 A_8^4 A}{A_3^4} - \frac{30A_7 A_8^2 A^2 \bar{A}}{A_3^2} + \frac{4A_6 A_8^3 A}{A_3^3} + \frac{12A_6 A_8 A^2 \bar{A}}{A_3} - 10A_7 A^3 \bar{A}^2 = 0 \tag{68}$$

It is appropriate that A, expressed as a polar state:

$$A = \frac{1}{2} a(\tau_2) e^{i\beta(\tau_2)} \tag{69}$$

where a and β are the real function of τ_2. Substituting (90) into (89) and separating the result into real and imaginary parts, we obtain:

$$\dot{a}(\tau_2) = 0, \tag{70}$$

$$\dot{\beta} = \frac{\tau_2}{-\sqrt{A_3} a} \times \left(-\frac{3}{8} A_5 a^3 - \frac{1}{2} a A_1 A_8 + \frac{A_2 A_8^2 a}{2A_3} + \frac{3}{8} a^3 A_2 A_3 + \frac{A_4 A_8 a}{A_3} - \frac{3A_5 A_8^2 a}{2{A_3}^2} - \frac{5A_7 {A_8}^4 a}{2{A_3}^4} - \frac{30A_7 {A_8}^2 a^3}{8{A_3}^2} + \frac{2A_6 {A_8}^3 a}{{A_3}^3} + \frac{12A_6 A_8 a^3}{8A_3} - \frac{10}{32} A_7 a^5 \right) \tag{71}$$

where the dot ($\bullet$) denotes the derivative concerning to τ_2 . As $\dot{a}(\tau_2) = 0$ therefore a is a constant and

$$a(\tau_2) = a_0, \tag{72}$$

Please cite this article as: I. Karimipour, Y.T. Beni and A.H. Akbarzadeh, Size-dependent nonlinear forced vibration and dynamic stability of electrically actuated micro-plates, Commun Nonlinear Sci Numer Simulat, https://doi.org/10.1016/j.cnsns.2019.104856

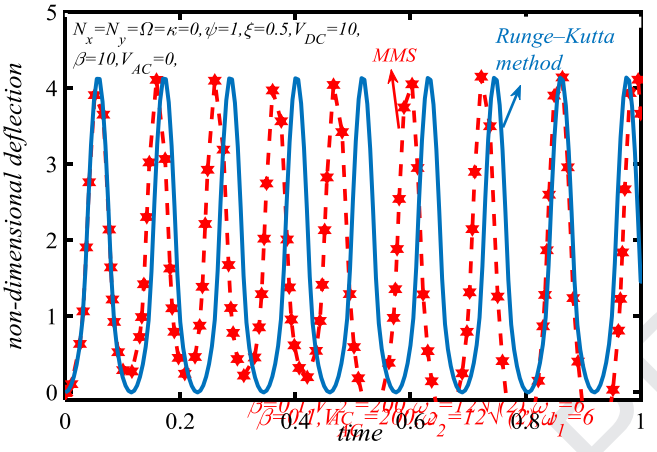

Fig. 6. Response of the micro-plate.

$$\beta = \frac{1}{-\sqrt{A_3}a}\times\left(-\frac{3}{8}A_5a^3-\frac{1}{2}aA_1A_8+\frac{A_2A_8^2a}{2A_3}+\frac{3}{8}a^3A_2A_3+\frac{A_4A_8a}{A_3}\right.$$
$$\left.-\frac{3A_5A_8^2a}{2{A_3}^2}-\frac{5A_7{A_8}^4a}{2{A_3}^4}-\frac{30A_7{A_8}^2a^3}{8{A_3}^2}+\frac{2A_6{A_8}^3a}{{A_3}^3}+\frac{12A_6A_8a^3}{8A_3}-\frac{10}{32}A_7a^5\right)\tau_2+\beta_0 \tag{73}$$

Here β_0 is a constant. Now using $\tau_2=\varepsilon^2 t$ we reach to:

$$A=\frac{1}{2}a_0\times\exp\left(i\frac{1}{-\sqrt{A_3}a}\left(-\frac{3}{8}A_5a^3-\frac{1}{2}aA_1A_8+\frac{A_2A_8^2a}{2A_3}+\frac{3}{8}a^3A_2A_3+\frac{A_4A_8a}{A_3}\right.\right.$$
$$\left.\left.-\frac{3A_5A_8^2a}{2{A_3}^2}-\frac{5A_7{A_8}^4a}{2{A_3}^4}-\frac{30A_7{A_8}^2a^3}{8{A_3}^2}+\frac{2A_6{A_8}^3a}{{A_3}^3}+\frac{12A_6A_8a^3}{8A_3}-\frac{10}{32}A_7a^5\right)\varepsilon^2t+\beta_0 i\right) \tag{74}$$

Substituting Eq. (74) in the expressions for R_0, i.e., Eq. (64) one obtains:

$$R_0=-\frac{A_8}{A_3}+a_0\times\cos\left(\sqrt{A_3}\tau_0+\frac{1}{-\sqrt{A_3}a}\left(-\frac{3}{8}A_5a^3-\frac{1}{2}aA_1A_8+\frac{A_2A_8^2a}{2A_3}\right.\right.$$
$$+\frac{3}{8}a^3A_2A_3+\frac{A_4A_8a}{A_3}+\frac{3}{8}a^3A_2A_3+\frac{A_4A_8a}{A_3}-\frac{3A_5{A_8}^2a}{2{A_3}^2}-\frac{5A_7{A_8}^4a}{2{A_3}^4}$$
$$\left.\left.-\frac{30A_7{A_8}^2a^3}{8{A_3}^2}+\frac{2A_6{A_8}^3a}{{A_3}^3}+\frac{12A_6A_8a^3}{8A_3}-\frac{10}{32}A_7a^5\right)\tau_2+\beta_0\right) \tag{75}$$

By replacing $t=0$ in the relation (75), the equation of the static deflection and with derivative from the relation (75), and setting $t=0$, the relation of the initial velocity is obtained. Now, if the time tends to the infinitely, in other words $\tau_i\to\infty$, $i=1,2$, Eq. (75) only has a mathematically meaning that a_0 goes to zero ($a_0\to 0$). The remainder relationship is independent of time, indicating the maximum deflection of the micro-plate.

$$w_{\max}=-\frac{A_8}{A_3} \tag{76}$$

Fig. 6 shows the comparison between the response of Multiple scales method (MMS) and Runge–Kutta method with displacement and initial velocity of zero. As can be seen, the results of non-dimensional deflection obtained by Runge–kutta method with respect to time are in good agreement with the findings results presented by MMS.

5.4. Dynamic response of rectangular micro-plate under electrical excitation

In this section, the dynamic response of rectangular micro-plate under electrical excitation, consisting of DC constant and alternating AC voltages are studied. DC Voltage component causes to bend micro-plate to a new position. Then the AC voltage causes vibration the micro-plate around the new equilibrium point. Such structures are used in resonator microscopes. Obtaining a frequency response curve in primary and secondary resonance modes and investigating instability dynamics

(pull-in) are the goals of this section. First, the system's response to the electric voltage in the primary resonance is studied by the method of multiple scales. In the following, the dynamic behavior of the micro-plate under Subharmonic and Superharmonic resonance conditions are also studied. In this section, it is supposed that the micro-plate shown in Fig. 1 is excited by an electrical voltage $V(t) = V_{DC} + V_{AC}\cos(\Omega t)$, where V_{DC} is the constant voltage, V_{AC} is the amplitude of variable voltage and Ω is the excitation frequency.

5.4.1. Primary resonance using multiple scale method considering a weak forcing function

In the primary resonance state, the excitation force frequency is very close to the fundamental natural frequency of the system. As discussed in the previous section, in the absence of external force, the amplitude of free vibration response is a function of the natural frequency (ω_0). Similar to the linear vibration here we may consider the behavior of the micro-plate near the resonance condition, i.e., when the external frequency is equal to the natural frequency of the system. This condition is known as the primary resonance condition ($\Omega \approx \omega_0$). To study the behavior of the system near the primary resonance condition, one may use the detuning parameter which represents the nearness of the external frequency to that of the natural frequency. Hence one may write:

$$\Omega = \omega_0 + \varepsilon^2\sigma \tag{77}$$

where Ω is the excitation frequency and ω_0 is the linear natural frequency of the system. σ is the detuning parameter that indicates the proximity of the excited frequency to the linear frequency of the system. In the primary resonance condition, the amplitude of the excitation force is considered the same order as the nonlinear terms. Therefore, the excitation voltage is sorted as follows.

$$V(t) = V_{DC} + \varepsilon^2 V_{AC}\cos(\Omega t) \tag{78}$$

As a result, Eq. (56) found the form as follows:

$$\begin{aligned}&\ddot{R}(t) + A_3R(t) + A_9\left(V_{DC} + \varepsilon^2 V_{AC}\cos(\Omega t)\right)^2 + \varepsilon^2\left(A_1R(t)\ddot{R}(t)\right.\\&\left.+A_2R(t)^2\ddot{R}(t) + A_4R(t)^2 + A_5R(t)^3 + A_6R(t)^4 + A_7R(t)^5\right) = 0,\\&A_9 = -\frac{16\beta}{9}\end{aligned} \tag{79}$$

In this analysis, it is assumed that ${V_{DC}}^2 >> {V_{AC}}^2$. Substituting Eq. (60) in Eq. (79) moreover, separate terms with a different order of ε, one obtains the following equations.

$$O\left(\varepsilon^0\right) : D_0^2R_0 + A_3R_0 = -A_9{V^2}_{DC} \tag{80}$$

$$O\left(\varepsilon^1\right) : D_0^2R_1 + A_3R_1 = -2D_0D_1R_0 \tag{81}$$

$$\begin{aligned}O\left(\varepsilon^2\right) : &D_0^2R_2 + A_3R_2 = -2D_0D_1R_1 - 2D_0D_2R_0 - D_1^2R_0\\&- A_1R_0D_0^2R_0 - A_2R_0^2D_0^2R_0 - A_4R_0^2 - A_5R_0^3 - A_6R_0^4 - A_7R_0^5\\&- 2A_9V_{AC}V_{DC}\cos(\Omega t)\end{aligned} \tag{82}$$

The general solution for the Eq. (80) is as follows:

$$R_0 = -\frac{A_9{V^2}_{DC}}{A_3} + A(\tau_1,\tau_2)e^{i\sqrt{A_3}\tau_0} + \bar{A}(\tau_1,\tau_2)e^{-i\sqrt{A_3}\tau_0} \tag{83}$$

By substituting Eq. (83) in Eq. (81) one obtains the following equation.

$$D_0^2R_1 + A_3R_1 = -2i\sqrt{A_3}D_1A(\tau_1,\tau_2)e^{i\sqrt{A_3}\tau_0} + 2i\sqrt{A_3}D_1\bar{A}(\tau_1,\tau_2)e^{-i\sqrt{A_3}\tau_0} \tag{84}$$

By solving Eq. (84), one can write

$$R_1 = B(\tau_1,\tau_2)e^{i\sqrt{A_3}\tau_0} + \bar{B}(\tau_1,\tau_2)e^{-i\sqrt{A_3}\tau_0} \tag{85}$$

By replacing (83), (85) and (77) into the Eq. (82); the following equation is obtained.

$$\begin{aligned}D_0^2R_2 + A_3R_2 = CC + O.H.T + e^{i\omega_0 t}\times\Bigg(&-2i\sqrt{A_3}D_1B - 2i\sqrt{A_3}D_2A - 3A_5A^2\bar{A}\\&- A_1A_9AV_{DC}^2 + \frac{A_2A_9^2V_{DC}^2A}{A_3} + 3A_2A_3A^2\bar{A} + \frac{2A_4A_9V_{DC}^2A}{A_3} - \frac{3A_5A_9^2V_{DC}^4A}{A_3^2}\\&- \frac{5A_7A_9^4V_{DC}^8A}{A_3^4} - \frac{30A_7A_9^2V_{DC}^4A^2\bar{A}}{A_3^2} + \frac{4A_6A_9^3AV_{DC}^6}{A_3^3} + \frac{12A_6A_9V_{DC}^2A^2\bar{A}}{A_3}\end{aligned}$$

Please cite this article as: I. Karimipour, Y.T. Beni and A.H. Akbarzadeh, Size-dependent nonlinear forced vibration and dynamic stability of electrically actuated micro-plates, Commun Nonlinear Sci Numer Simulat, https://doi.org/10.1016/j.cnsns.2019.104856

$$- 10A_7A^3\bar{A}^2 - A_9V_{AC}V_{DC}e^{i\sigma\tau_2}\Big) \tag{86}$$

To eliminate the secular and near secular terms from Eq. (86), one can write:

$$-2i\sqrt{A_3}D_2A - 3A_5A^2\bar{A} - A_1A_9AV_{DC}^2 + \frac{A_2A_9^2V_{DC}^2A}{A_3} + 3A_2A_3A^2\bar{A} + \frac{2A_4A_9V_{DC}^2A}{A_3} - \frac{3A_5A_9^2V_{DC}^4A}{A_3^2} - \frac{5A_7A_9^4V_{DC}^8A}{A_3^4} - \frac{30A_7A_9^2V_{DC}^4A^2\bar{A}}{A_3^2} + \frac{4A_6A_9^3V_{DC}^6A}{A_3^3} + \frac{12A_6A_9V_{DC}^2A^2\bar{A}}{A_3} - 10A_7A^3\bar{A}^2 - A_9V_{AC}V_{DC}e^{i\sigma\tau_2} = 0 \tag{87}$$

It follows that B is only a function of τ_2. Now by substituting $A = \frac{1}{2}a(\tau_2)e^{i\beta(\tau_2)}$ in Eq. (87) moreover, separating the real and imaginary parts, following reduced equations are obtained.

$$\dot{a} = \frac{-A_9V_{AC}V_{DC}}{\sqrt{A_3}}\sin(\sigma\tau_2 - \beta), \tag{88}$$

$$a\dot{\beta} = \frac{1}{-\sqrt{A_3}}\left\{\left(-\frac{1}{2}A_1A_9V_{DC}^2 + \frac{1}{2}\frac{A_2A_9^2V_{DC}^2}{A_3} + \frac{A_4A_9V_{DC}^2}{A_3} - \frac{3}{2}\frac{A_5A_9^2V_{DC}^4}{{A_3}^2} - \frac{5}{2}\frac{A_7{A_9}^4V_{DC}^8}{{A_3}^4} + \frac{2A_6{A_9}^3V_{DC}^6}{{A_3}^3}\right)a + \left(-\frac{3}{8}A_5 - \frac{30}{8}\frac{A_7{A_9}^2V_{DC}^4}{{A_3}^2} + \frac{12}{8}\frac{A_6A_9V_{DC}^2}{A_3} + \frac{3}{8}A_2A_3\right)a^3 - \frac{10}{32}A_7a^5 - A_9V_{AC}V_{DC}\cos(\sigma\tau_2 - \beta)\right\} \tag{89}$$

To write these two equations in its autonomous form one may use $\gamma = \sigma\tau_2 - \beta$ and obtained the following equations.

$$\dot{a} = \frac{-A_9V_{AC}V_{DC}}{\sqrt{A_3}}\sin(\gamma), \tag{90}$$

$$a\dot{\gamma} = a\sigma + \frac{1}{\sqrt{A_3}}\left(\left(-\frac{1}{2}A_1A_9V_{DC}^2 + \frac{1}{2}\frac{A_2A_9^2V_{DC}^2}{A_3} + \frac{A_4A_9V_{DC}^2}{A_3} - \frac{3}{2}\frac{A_5A_9^2V_{DC}^4}{{A_3}^2} - \frac{5}{2}\frac{A_7{A_9}^4V_{DC}^8}{{A_3}^4} + \frac{2A_6{A_9}^3V_{DC}^6}{{A_3}^3}\right)a + \left(-\frac{3}{8}A_5 - \frac{30}{8}\frac{A_7{A_9}^2V_{DC}^4}{{A_3}^2} + \frac{12}{8}\frac{A_6A_9V_{DC}^2}{A_3} + \frac{3}{8}A_2A_3\right)a^3 - \frac{10}{32}A_7a^5 - A_9V_{AC}V_{DC}\cos(\gamma)\right) \tag{91}$$

One should solve these two equations to obtain a and γ. Now for the steady state as $\dot{a}$ and $\dot{\gamma}$ equals to 0, one can write Eqs. (90) and (91) as:

$$\frac{-A_9V_{AC}V_{DC}}{\sqrt{A_3}}\sin(\gamma) = 0, \tag{92}$$

$$a\sqrt{A_3}\sigma + \left(-\frac{1}{2}A_1A_9V_{DC}^2 + \frac{1}{2}\frac{A_2A_9^2V_{DC}^2}{A_3} + \frac{A_4A_9V_{DC}^2}{A_3} - \frac{3}{2}\frac{A_5A_9^2V_{DC}^4}{{A_3}^2} - \frac{5}{2}\frac{A_7{A_9}^4V_{DC}^8}{{A_3}^4} + \frac{2A_6{A_9}^3V_{DC}^6}{{A_3}^3}\right)a + \left(-\frac{3}{8}A_5 - \frac{30}{8}\frac{A_7{A_9}^2V_{DC}^4}{{A_3}^2} + \frac{12}{8}\frac{A_6A_9V_{DC}^2}{A_3} + \frac{3}{8}A_2A_3\right)a^3 - \frac{10}{32}A_7a^5 = A_9V_{AC}V_{DC}\cos(\gamma) \tag{93}$$

Now eliminating γ from the above equations, one obtains:

$$\sigma = \frac{1}{a\sqrt{A_3}} \times \left(\pm A_9V_{AC}V_{DC} - \left(\left(-\frac{1}{2}A_1A_9V_{DC}^2 + \frac{1}{2}\frac{A_2A_9^2V_{DC}^2}{A_3} + \frac{A_4A_9V_{DC}^2}{A_3} - \frac{3}{2}\frac{A_5A_9^2V_{DC}^4}{{A_3}^2} - \frac{5}{2}\frac{A_7{A_9}^4V_{DC}^8}{{A_3}^4}\right)a + \left(-\frac{3}{8}A_5 - \frac{30}{8}\frac{A_7{A_9}^2V_{DC}^4}{{A_3}^2} + \frac{12}{8}\frac{A_6A_9V_{DC}^2}{A_3}\right.\right.\right.$$

Please cite this article as: I. Karimipour, Y.T. Beni and A.H. Akbarzadeh, Size-dependent nonlinear forced vibration and dynamic stability of electrically actuated micro-plates, Commun Nonlinear Sci Numer Simulat, https://doi.org/10.1016/j.cnsns.2019.104856

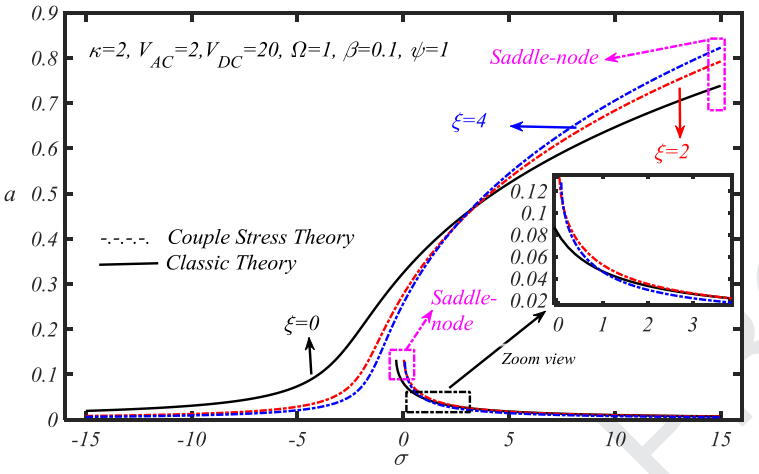

Fig. 7. Frequency response curve of a rectangular micro-plate for different values of ξ.

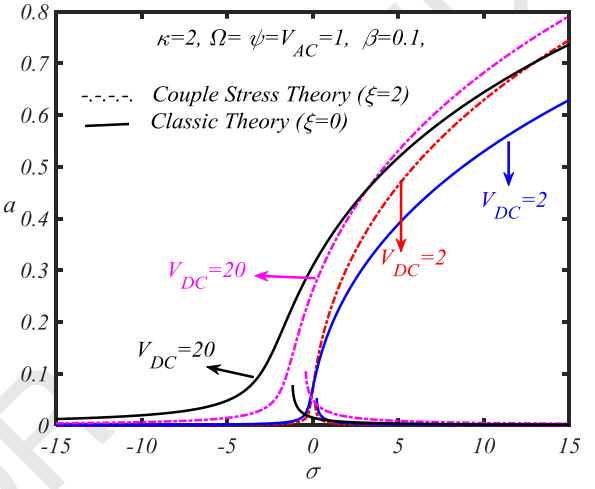

Fig. 8. Frequency response curve of a rectangular micro-plate for different values of V_{DC}.

$$+\frac{3}{8}A_2A_3\Big)a^3+\frac{4A_6{A_9}^3V_{DC}^6}{{A_3}^3}-\frac{10}{32}A_7a^5\Big)\Big) \tag{94}$$

The frequency response curve of a rectangular micro-plate for $V_{DC}=20$, $V_{AC}=2$ is given in Fig. 7.

As can be seen, the existence of nonlinear terms in the governing equation leads to appearance plate stiffness property. The saddle-node bifurcation points have been shown in Fig. 7. To identify the pull-in dynamic voltage, the AC voltage response should be calculated. For this purpose, the amplitude range of the vibration should be plotted in terms of the excited amplitude. With increasing the voltage when the excitation voltage reaches to pull-in dynamic voltage, a sudden change in the amplitude of the vibration is observed. This sudden change in the vibration amplitude can be so high, that leads to a collision of a capacitor micro-plate with the fixed electrode. Therefore, for the design of such systems, it is necessary to care about critical voltage. It should be noted that, due to assumption (${V_{DC}}^2 >> {V_{AC}}^2$), so by increasing AC voltage, this assumption can cause many errors in the semi-analytical response. However, in a low value of V_{AC} the proposed method is an appropriate method. Fig. 8 shows the frequency response curve of a rectangular micro-plate for different DC voltages. According to this figure with increasing constant voltage (V_{DC}) stiffness of the micro-plate becomes less.

Fig. 9 shows the frequency response curve of a rectangular micro-plate for a DC voltage $V_{DC}=20(Volt)$ and different AC voltages.

Regarding Fig. 9, it can be seen that with increasing the alternating voltage, V_{AC} the branches of each curve get more spaced apart. In other words, the voltages, V_{AC}, does not have any effect on the level of stiffness of the micro-plate and only acts as an external excitation dynamic force. Fig. 10 shows the frequency response curve of a rectangular micro-plate for the AC voltage $V_{AC}=2\ volt$ and DC voltage $V_{DC}=20\ volt$, for the different value of κ. According to this figure, it can be seen that the reduction of the non-dimensional parameter κ reduces the stiffness of the micro-plate as it has already been mentioned

Please cite this article as: I. Karimipour, Y.T. Beni and A.H. Akbarzadeh, Size-dependent nonlinear forced vibration and dynamic stability of electrically actuated micro-plates, Commun Nonlinear Sci Numer Simulat, https://doi.org/10.1016/j.cnsns.2019.104856

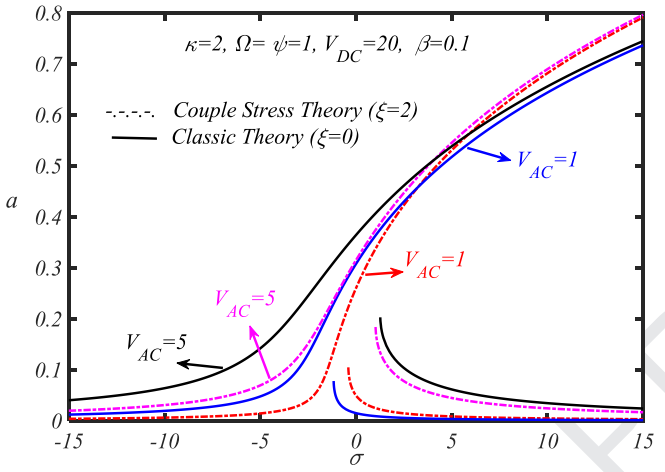

Fig. 9. Frequency response curve of a rectangular micro-plate for different values of V_{AC}.

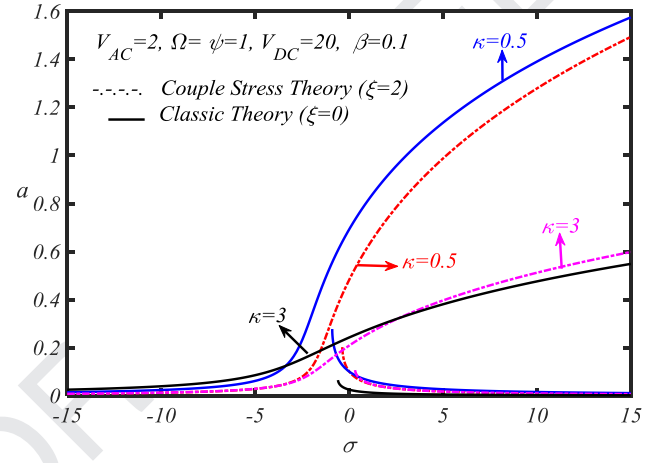

Fig. 10. Frequency response curve of a rectangular micro-plate for different values of κ.

for the static case (Fig. 5). In other words, reducing κ reduces the effect of the stretch of the mid-plane and the stiffness of the micro-plate.

Fig. 11 indicates the frequency response curve of a rectangular micro-plate for different values of ψ. According to this figure, a significant change in the frequency response curve is observed with decreasing ψ from 3 to 1.

Fig. 12 shows the vibration amplitude curve according to the amplitude of the excitation force for a rectangular micro-plate for different values of σ. As seen it turns out that for positive values of σ for a given alternating voltage, there are several values for the vibration amplitude. However, for negative values of σ for an alternating voltage, there are not multiple values for the vibration amplitude. On the other hand, for positive values of σ by increasing σ, an increase in the critical dynamic voltage occurs. For instance, in the two cases of modified couple stress theory, pull-in voltages are as follow:

$\sigma = 3; \{^{a = 0.222}_{V_{AC,PI} = 18.13}$ and, $\sigma = 1; \{^{a = 0.138}_{V_{AC,PI} = 4.40}$. As a significant result, it can be stated that for a specific DC voltage, the critical dynamic voltage is a function of the forced excitation frequency. The effect of the mid-plane stretching on critical dynamic voltage is now investigated in Fig. 13.

This figure shows vibration amplitude in terms of the excitation force amplitude for different values of κ. As can be seen, with increasing κ, the critical dynamic voltage decreases. Previously mentioned that κ is the value of the stretch of the mid-plane. Therefore, for a given excitation frequency $(\Omega = 1)$, the increase in the κ decreases the critical dynamic voltage.

Fig. 14 shows the vibration amplitude curve according to the amplitude of the excitation force for different values of ψ. As can be seen, by increasing ψ, the critical dynamic voltage $(V_{AC(Pull-in)})$ decreases.

Please cite this article as: I. Karimipour, Y.T. Beni and A.H. Akbarzadeh, Size-dependent nonlinear forced vibration and dynamic stability of electrically actuated micro-plates, Commun Nonlinear Sci Numer Simulat, https://doi.org/10.1016/j.cnsns.2019.104856

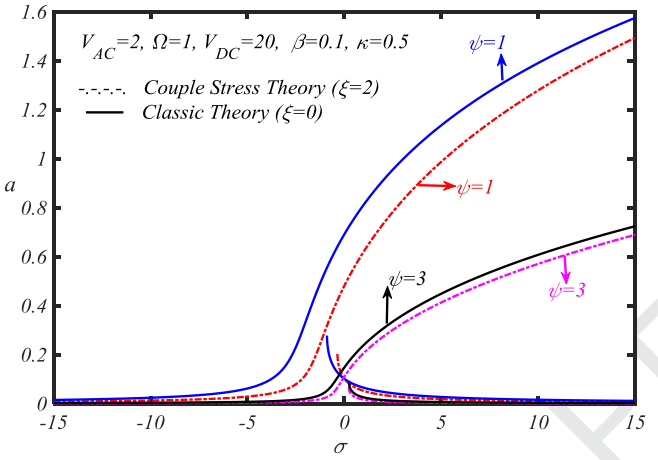

Fig. 11. Frequency response curve of a rectangular micro-plate for different values of ψ.

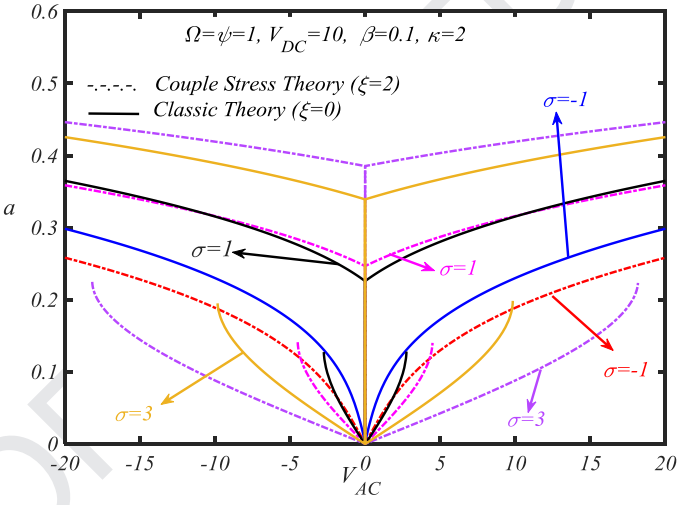

Fig. 12. Vibration amplitude curve of a rectangular micro-plate for different values of σ.

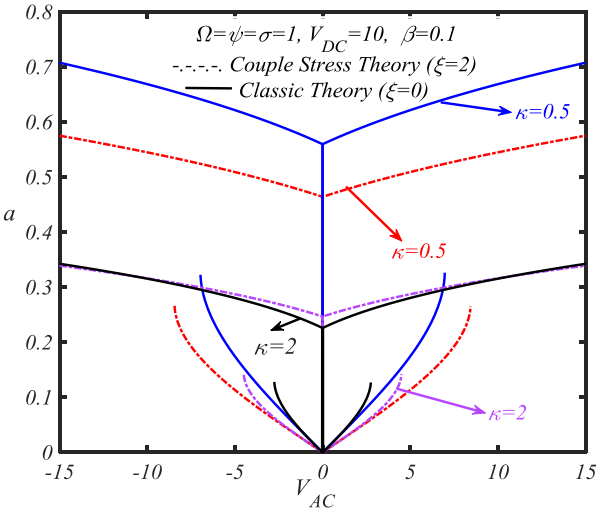

Fig. 13. Vibration amplitude in terms of the excitation force amplitude for a rectangular micro-plate for different values of κ.

Please cite this article as: I. Karimipour, Y.T. Beni and A.H. Akbarzadeh, Size-dependent nonlinear forced vibration and dynamic stability of electrically actuated micro-plates, Commun Nonlinear Sci Numer Simulat, https://doi.org/10.1016/j.cnsns.2019.104856

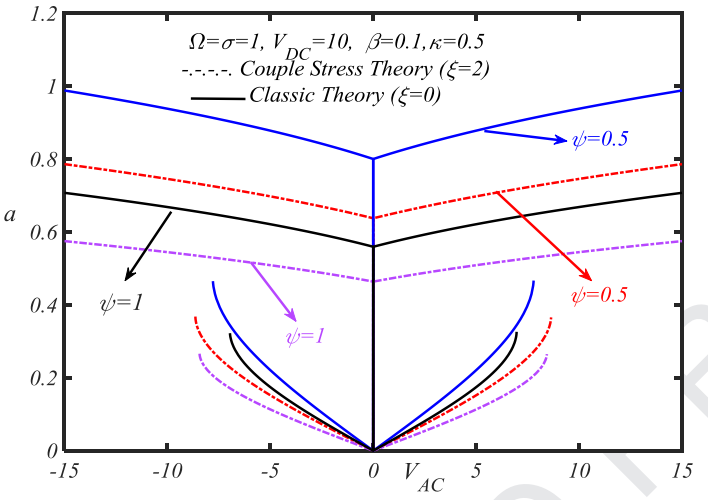

Fig. 14. Vibration amplitude in terms of the excitation force amplitude for a rectangular micro-plate for different values of ψ.

5.4.2. Secondary resonance

In the secondary resonance, the domain of excitation load is not assumed to be small [62], i.e., the forcing term is assumed to be of same the order as that of the linear term. So, the equation of motion considered in this case as:

$$\ddot{R}(t)+A_3R(t)+\varepsilon\left(A_1R(t)\ddot{R}(t)+A_2R(t)^2\ddot{R}(t)+A_4R(t)^2+A_5R(t)^3+A_6R(t)^4+A_7R(t)^5\right)$$
$$=-A_9(V_{DC}+V_{AC}\cos(\Omega t))^2 \tag{95}$$

Using the method of multiple scales, the solution of Eq. (95) can be written as:

$$R(\tau_0,\tau_1,\varepsilon)=R_0(\tau_0,\tau_1,)+\varepsilon R_1(\tau_0,\tau_1) \tag{96}$$

Now by separating the terms with a different order of ε, one obtains the following equations:

$$O\left(\varepsilon^0\right):D_0^2R_0+A_3R_0=-A_9(V_{DC}+V_{AC}\cos(\Omega t))^2 \tag{97}$$

$$O\left(\varepsilon^1\right):D_0^2R_1+A_3R_1=-2D_0D_1R_0-A_1R_0D_0^2R_0-A_2Z_0^2D_0^2R_0$$
$$-A_4R_0^2-A_5R_0^3-A_6R_0^4-A_7R_0^5 \tag{98}$$

The solution of Eq. (97) can be written as:

$$R_0=-\frac{A_9V_{DC}^2}{2A_3}+A(\tau_1)e^{i\omega_0\tau_0}+\Lambda e^{i\Omega\tau_0}+CC \tag{99}$$

where

$$\omega_0=\sqrt{A_3}\ ,\quad \Lambda=-\frac{A_9V_{DC}V_{AC}}{\left(\omega_0^2-\Omega^2\right)} \tag{100}$$

It may be noted that unlike the previous section, where only the complementary part of the solution was present, in this case, both complimentary and particular integral parts, are present in the solution of R_0. It may be noted that when the exponent terms of the mixed secular terms are equal to ω_0 a resonance condition will occur. Hence, resonance will be observed in the system when;$\{$ $\Omega=\omega_0$, (Primary resonance) $\Omega=3\omega_0$, (Sub harmonic resonance) . $3\Omega=\omega_0$, (Superharmonic Resonance)

5.4.3. Superharmonic resonance

To express the nearness of the external excitation frequency to one-third of the natural frequency one may use the detuning parameter $\Omega\approx\frac{1}{3}\omega_0$ as follows:

$$3\Omega=\omega_0+\sigma\varepsilon \tag{101}$$

Now to eliminate the secular and near secular terms from Eq. (98) one can write:

$$-A_5\Lambda^3e^{i\varepsilon\sigma\tau_0}-2i\omega_0D_1A+A_2\Lambda^3\Omega^2e^{i\varepsilon\sigma\tau_0}-6A_5A\Lambda^2-3A_5A^2\bar{A}+3A_2A^2\bar{A}\omega^2$$
$$-\frac{10A_7A_9^2V_{DC}^4\Lambda^3e^{i\varepsilon\sigma\tau_0}}{A_3^2}-\frac{60A_7A_9^2V_{DC}^4A\Lambda^2}{A_3^2}-\frac{3A_5A_9^2V_{DC}^4A}{A_3^2}-60A_7A^2\bar{A}\Lambda^2$$

Please cite this article as: I. Karimipour, Y.T. Beni and A.H. Akbarzadeh, Size-dependent nonlinear forced vibration and dynamic stability of electrically actuated micro-plates, Commun Nonlinear Sci Numer Simulat, https://doi.org/10.1016/j.cnsns.2019.104856

$$+\frac{2A_4A_9V_{DC}^4A}{A_3}+\frac{12A_6A_9V_{DC}^2A^2\bar{A}}{A_3}+\frac{4A_6A_9V_{DC}^2\Lambda^3e^{i\varepsilon\sigma\tau_0}}{A_3}-10A_7A^3\bar{A}^2$$
$$-\frac{5A_7A_9{}^4V_{DC}^8A}{A_3{}^4}-30A_7A\Lambda^4+\frac{24A_6A_9V_{DC}^2A\Lambda^2}{A_3}+4A_2A\Lambda^2\Omega^2$$
$$+2A_2A\Lambda^2\omega_0^2+\frac{A_2A_9{}^2V_{DC}^4A\omega_0^2}{A_3{}^2}-5A_7\Lambda^5e^{i\varepsilon\sigma\tau_0}=0 \tag{102}$$

Using $A=\frac{1}{2}a(\tau_1)e^{i\beta(\tau_1)}$ and separating the real and imaginary parts following reduced equations are obtained.

$$\dot{a}=\frac{1}{\omega_0}\left(-A_5\Lambda^3+A_2\Lambda^3\Omega^2-\frac{10A_7A_9^2V_{DC}^4\Lambda^3}{A_3{}^2}+\frac{4A_6A_9V_{DC}^2\Lambda^3}{A_3}-5A_7\Lambda^5\right)\times$$
$$\sin(\sigma\tau_1-\beta)=0, \tag{103}$$

$$a\dot{\beta}=\frac{\cos(\sigma\tau_1-\beta)}{-\omega_0}\left(\left(-A_5\Lambda^3+A_2\Lambda^3\Omega^2-\frac{10A_7A_9^2V_{DC}^4\Lambda^3}{A_3{}^2}+\frac{4A_6A_9V_{DC}^2\Lambda^3}{A_3}-5A_7\Lambda^5\right)\right.$$
$$-3A_5a\Lambda^2-\frac{3}{8}A_5a^3\frac{30A_7A_9^2V_{DC}^4a\Lambda^2}{A_3{}^2}-\frac{3A_5A_9^2V_{DC}^4a}{2A_3{}^2}+\frac{3}{8}A_2a^3\omega_0^2+\frac{A_4A_9V_{DC}^2a}{A_3}$$
$$+\frac{12A_6A_9V_{DC}^2a^3}{8A_3}-\frac{60}{8}A_7a^3\Lambda^2-\frac{5A_7A_9^4V_{DC}^8a}{2A_3{}^4}-\frac{10}{32}A_7a^5-15A_7a\Lambda^4$$
$$\left.+\frac{12A_6A_9V_{DC}^2a\Lambda^2}{A_3}+2A_2a\Lambda^2\Omega^2+A_2a\Lambda^2\omega_0^2+\frac{A_2A_9^2V_{DC}^4a\omega_0^2}{2A_3{}^2}\right) \tag{104}$$

Now to express the above equations in their autonomous form one may use the following transformation., $\gamma=\sigma\tau_1-\beta$ Hence, Eq. (103) can be written as:

$$\dot{a}=\frac{\sin(\gamma)}{\omega_0}\times\left(-A_5\Lambda^3+A_2\Lambda^3\Omega^2-\frac{10A_7A_9^2V_{DC}^4\Lambda^3}{A_3{}^2}+\frac{4A_6A_9V_{DC}^2\Lambda^3}{A_3}-5A_7\Lambda^5\right), \tag{105}$$

$$a\dot{\gamma}=a\sigma+\frac{1}{\omega_0}\left(\left(-A_5\Lambda^3+A_2\Lambda^3\Omega^2-\frac{10A_7A_9^2V_{DC}^4\Lambda^3}{A_3{}^2}+\frac{4A_6A_9V_{DC}^2\Lambda^3}{A_3}\right.\right.$$
$$\left.-5A_7\Lambda^5\right)\cos(\sigma\tau_1-\beta)-3A_5a\Lambda^2-\frac{3}{8}A_5a^3\frac{30A_7A_9^2V_{DC}^4a\Lambda^2}{A_3{}^2}-\frac{3A_5A_9^2V_{DC}^4a}{2A_3{}^2}$$
$$+\frac{3}{8}A_2a^3\omega_0^2+\frac{A_4A_9V_{DC}^2a}{A_3}+\frac{12A_6A_9V_{DC}^2a^3}{8A_3}-\frac{60}{8}A_7a^3\Lambda^2-\frac{5A_7A_9^4V_{DC}^8a}{2A_3{}^4}-\frac{10}{32}A_7a^5$$
$$\left.-15A_7a\Lambda^4+\frac{12A_6A_9V_{DC}^2a\Lambda^2}{A_3}+2A_2a\Lambda^2\Omega^2+A_2a\Lambda^2\omega_0^2+\frac{A_2A_9^2V_{DC}^4a\omega_0^2}{2A_3{}^2}\right) \tag{106}$$

For steady state, the time derivative terms should be vanished, in Eq. (105) and (106), i.e., $\dot{a}=\dot{\gamma}=0$. Now by eliminating γ from the above two equations, one can obtain a closed-form equation which can be used for finding the frequency response of the system and the relation between the detuning parameter and the amplitude of the response as follows:

$$\sigma=-\frac{1}{a\omega_0}\left(\pm\left(-A_5\Lambda^3+A_2\Lambda^3\Omega^2-\frac{10A_7A_9^2V_{DC}^4\Lambda^3}{A_3{}^2}+\frac{4A_6A_9V_{DC}^2\Lambda^3}{A_3}-5A_7\Lambda^5\right)\right.$$
$$+\left(-3A_5a\Lambda^2-A_5a^3\frac{90A_7A_9^2V_{DC}^4a\Lambda^2}{8A_3{}^2}-\frac{3A_5A_9^2V_{DC}^4a}{2A_3{}^2}+\frac{3}{8}A_2a^3\omega_0^2+\frac{A_4A_9V_{DC}^2a}{A_3}\right.$$
$$+\frac{12A_6A_9V_{DC}^2a^3}{8A_3}-\frac{60A_7a^3\Lambda^2}{8}-\frac{5A_7A_9^4V_{DC}^8a}{2A_3{}^4}-\frac{10A_7a^5}{32}-15A_7a\Lambda^4$$
$$\left.\left.+\frac{12A_6A_9V_{DC}^2a\Lambda^2}{A_3}+2A_2a\Lambda^2\Omega^2+A_2a\Lambda^2\omega_0^2+\frac{A_2A_9^2V_{DC}^4a\omega_0^2}{2A_3{}^2}\right)\right) \tag{107}$$

Hence, in this resonance condition, the nonlinearity adjusts the frequency of the free oscillation term to precisely three times the frequency of the excitations so that the response is periodic. Since the frequency of the free oscillation term is three times the frequency of excitation, such resonances are called superharmonic resonances [62]. Fig. 15 shows the frequency response curve of a micro-plate under electric voltage under superharmonic resonance state for different values of κ.

According to the above figure, it can be seen that by increasing the values of κ result in decreases the region in the frequency response curve. Also, with changing κ in large values of σ, the slip of frequency response diagrams does not change. It should be noted that by increasing κ the backbone curve tends to be moved to the right side.

Please cite this article as: I. Karimipour, Y.T. Beni and A.H. Akbarzadeh, Size-dependent nonlinear forced vibration and dynamic stability of electrically actuated micro-plates, Commun Nonlinear Sci Numer Simulat, https://doi.org/10.1016/j.cnsns.2019.104856

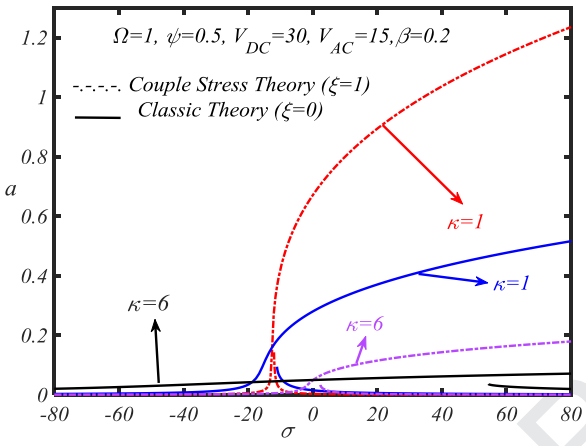

Fig. 15. Frequency response curve of a micro-plate under electric voltage and superharmonic resonance state for different values of κ.

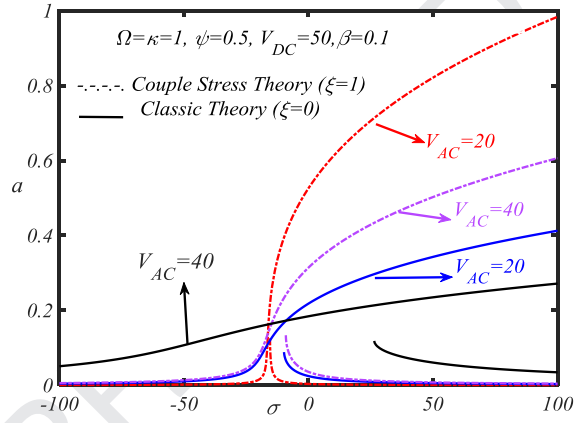

Fig. 16. Frequency response curve of a micro-plate under electric voltage and superharmonic resonance state for different values of V_{AC}.

Fig. 16. shows the frequency response curve of a micro-plate under electric voltage in superharmonic resonance state for different V_{AC} values. It can be seen that by increasing the values of V_{AC} result in decreases the region in the frequency response curve. Also, for any values of V_{AC}, the slip of frequency response diagrams does not change. This trend means that changing the AC voltage (V_{AC}) does not affect the stiffness of the micro-plate.

Fig. 17. shows the frequency response curve of a micro-plate under electric voltage in superharmonic resonance state for different V_{DC} values. It should be noted that by increasing V_{DC} stiffness of the micro-plate reduced, and the backbone curve tends to be moved to the right side.

5.4.4. Subharmonic resonance

When the external frequency is nearly three times the natural frequency of the system, using detuning parameter one can write

$$\Omega = 3\omega_0 + \sigma\varepsilon \tag{108}$$

Using a similar procedure of the multiple scale method, eliminating the secular terms from Eq. (98) one can write:

$$\begin{aligned}
&-3A_5A^2\bar{A} - 6A_5A\Lambda^2 - \frac{A_1A_9V_{DC}^2A\omega_0^2}{A_3} + 4A_2A\Lambda^2\Omega^2 + \frac{4A_6{A_9}^3V_{DC}^6A}{{A_3}^3}\\
&+ \frac{12A_6A_9V_{DC}^2A^2\bar{A}}{A_3} + \frac{24A_6A_9V_{DC}^2A\Lambda^2}{A_3} + \frac{12A_6A_9V_{DC}^2\bar{A}^2\Lambda e^{i\varepsilon\sigma\tau_0}}{A_3} + 2A_2\bar{A}^2\Lambda\omega_0^2e^{i\varepsilon\sigma\tau_0}\\
&- 60A_7A^2\bar{A}\Lambda^2 - \frac{3A_5{A_9}^2V_{DC}^4A}{{A_3}^2} + \frac{2A_4A_9V_{DC}^2A}{A_3} + \frac{A_2{A_9}^2V_{DC}^4A\omega_0^2}{{A_3}^2} - 30A_7A\Lambda^4\\
&- 10A_7A^3\bar{A}^2 - 2i\omega_0D_1A - 20A_7A\bar{A}^3\Lambda e^{i\varepsilon\sigma\tau_0} + A_2\bar{A}^2\Lambda\Omega^2e^{i\varepsilon\sigma\tau_0} + 3A_2A^2\bar{A}\omega_0^2
\end{aligned}$$

Please cite this article as: I. Karimipour, Y.T. Beni and A.H. Akbarzadeh, Size-dependent nonlinear forced vibration and dynamic stability of electrically actuated micro-plates, Commun Nonlinear Sci Numer Simulat, https://doi.org/10.1016/j.cnsns.2019.104856

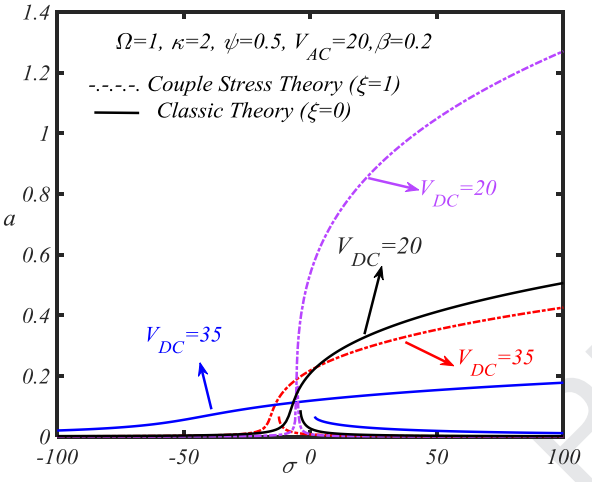

Fig. 17. Frequency response curve of a micro-plate under electric voltage and superharmonic resonance state for different values of V_{DC}.

$$+2A_2\Lambda^2 A\omega_0^2-\frac{5A_7{A_9}^4V_{DC}^8A}{{A_3}^4}-\frac{30A_7{A_9}^2V_{DC}^4A^2\bar{A}}{{A_3}^2}-\frac{60A_7{A_9}^2V_{DC}^4\Lambda^2A}{{A_3}^2}$$
$$-\frac{30A_7{A_9}^2V_{DC}^4\bar{A}^2\Lambda e^{i\varepsilon\sigma\tau_0}}{{A_3}^2}-3A_5\bar{A}^2\Lambda e^{i\varepsilon\sigma\tau_0}-30A_7\bar{A}^2\Lambda^3e^{i\varepsilon\sigma\tau_0}=0 \tag{109}$$

Using $A=\frac{1}{2}a(\tau_2)e^{i\beta(\tau_2)}$ and separating the real and imaginary parts following reduced equations are obtained. To express the obtained equations in their autonomous form one may use the $\gamma=\sigma\tau_1-3\beta$ transformation.

$$\dot{a}=\frac{\sin\gamma}{\omega_0}\times\left(\frac{12A_6A_9V_{DC}^2a^2\Lambda}{4A_3}+\frac{2}{4}A_2a^2\Lambda\omega_0^2-\frac{20}{16}A_7a^4\Lambda-\frac{3}{4}A_5a^2\Lambda-\right.$$
$$\left.\frac{30}{4}A_7a^2\Lambda^3+\frac{1}{4}A_2a^2\Lambda\Omega^2\frac{30A_7{A_9}^2V_{DC}^4a^2\Lambda}{4{A_3}^2}\right), \tag{110}$$

$$a\dot{\gamma}=a\sigma+\frac{3}{\omega_0}\times\left(-\frac{3A_5a^3}{8}-\frac{A_1A_9V_{DC}^2a\omega_0^2}{2A_3}+\frac{2A_6{A_9}^3V_{DC}^6a}{{A_3}^3}+\frac{12A_6A_9V_{DC}^2a^3}{8A_3}\right.$$
$$+2A_2a\Lambda^2\Omega^2+\frac{24A_6A_9V_{DC}^2a\Lambda^2}{2A_3}-\frac{60}{8}A_7a^3\Lambda^2-\frac{3A_5{A_9}^2V_{DC}^4a}{2{A_3}^2}-3A_5a\Lambda^2$$
$$+\frac{A_4A_9V_{DC}^2a}{A_3}+\frac{A_2{A_9}^2V_{DC}^4a\omega_0^2}{2{A_3}^2}-\frac{10A_7a^5}{32}+\frac{3A_2a^3\omega_0^2}{8}-15A_7a\Lambda^4+A_2\Lambda^2a\omega_0^2$$
$$-\frac{5A_7{A_9}^4V_{DC}^8a}{2{A_3}^4}-\frac{30A_7{A_9}^2V_{DC}^4a^3}{8{A_3}^2}-\frac{60A_7{A_9}^2V_{DC}^4\Lambda^2a}{2{A_3}^2}+\left(\frac{12A_6A_9V_{DC}^2a^2\Lambda}{4A_3}+\frac{A_2a^2\Lambda\omega_0^2}{2}\right.$$
$$\left.\left.-\frac{20}{16}A_7a^4\Lambda+\frac{1}{4}A_2a^2\Lambda\Omega^2\frac{30A_7{A_9}^2V_{DC}^4a^2\Lambda}{4{A_3}^2}-\frac{3}{4}A_5a^2\Lambda-\frac{30}{4}A_7a^2\Lambda^3\right)\cos\gamma\right) \tag{111}$$

For steady state, the time derivative terms should be vanished, in Eq. (110) and (111), i.e., $\dot{a}=\dot{\gamma}=0$. Now by eliminating γ from the above two equations, one can obtain a closed-form equation which can be used for finding the frequency response of the system:

$$\sigma=\frac{-3}{a\omega_0}\times\left(\pm\left(\frac{12A_6A_9V_{DC}^2a^2\Lambda}{4A_3}+\frac{A_2a^2\Lambda\omega_0^2}{2}-\frac{5A_7a^4\Lambda}{4}-\frac{3A_5a^2\Lambda}{4}\right.\right.$$
$$\left.+\frac{A_2a^2\Lambda\Omega^2}{4}\frac{30A_7{A_9}^2V_{DC}^4a^2\Lambda}{4{A_3}^2}-\frac{30A_7a^2\Lambda^3}{4}\right)-\frac{3A_5a^3}{8}-3A_5a\Lambda^2-\frac{A_1A_9V_{DC}^2a\omega_0^2}{2A_3}$$
$$+2A_2a\Lambda^2\Omega^2+\frac{2A_6{A_9}^3V_{DC}^6a}{{A_3}^3}+\frac{12A_6A_9V_{DC}^2a^3}{8A_3}+\frac{24A_6A_9V_{DC}^2a\Lambda^2}{2A_3}-\frac{60}{8}A_7a^3\Lambda^2$$
$$-\frac{3A_5{A_9}^2V_{DC}^4a}{2{A_3}^2}+\frac{A_4A_9V_{DC}^2a}{A_3}+\frac{A_2{A_9}^2V_{DC}^4a\omega_0^2}{2{A_3}^2}-15A_7a\Lambda^4-\frac{10A_7a^5}{32}+\frac{3A_2a^3\omega_0^2}{8}$$

Please cite this article as: I. Karimipour, Y.T. Beni and A.H. Akbarzadeh, Size-dependent nonlinear forced vibration and dynamic stability of electrically actuated micro-plates, Commun Nonlinear Sci Numer Simulat, https://doi.org/10.1016/j.cnsns.2019.104856

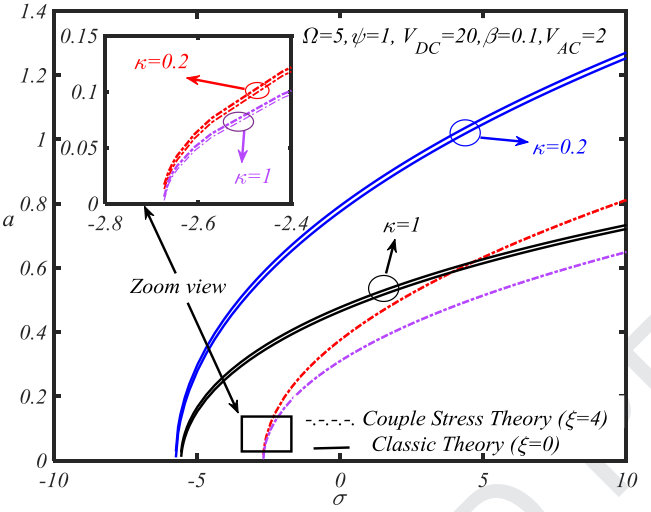

Fig. 18. Frequency Response curve of a micro-plate in subharmonic resonance conditions for various values of κ.

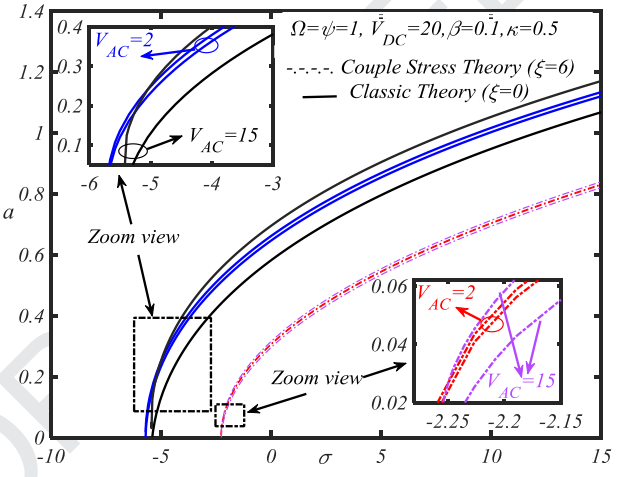

Fig. 19. Frequency response curve for a micro-plate under subharmonic resonance conditions for different V_{AC} values.

$$+A_2\Lambda^2 a\omega_0^2 - \frac{5A_7{A_9}^4V_{DC}^8 a}{2{A_3}^4} - \frac{30A_7{A_9}^2V_{DC}^4 a^3}{8{A_3}^2} - \frac{60A_7{A_9}^2V_{DC}^4\Lambda^2 a}{2{A_3}^2}\Bigg) \tag{112}$$

Above equation shows the system has a trivial state response (i.e., $a = 0$) and a non-trivial response. The frequency response curve of a micro-plate in subharmonic resonance conditions for various values of κ is shown in Fig. 18. From Fig. 18, it can be seen that by increasing the value of κ, the frequency response curves are shifted to the right side. The frequency response curve of a micro-plate under subharmonic resonance conditions for different V_{AC} values is shown in Fig. 19. According to this figure, it can be concluded that by increasing the Ac voltage (V_{AC}), the frequency response curves are closer to the vertical axis and the distance between the two branches of each curve will be greater. It is also observed that the increase in V_{AC} voltage does not affect the slope of the diagrams.

The frequency response curve of a micro-plate under AC voltage $V_{AC} = 5(vot)$ under subharmonic resonance conditions for different values of V_{DC} is shown in Fig. 20. As can be seen, increasing the V_{DC} voltage reduces the stiffness of the micro-plate.

6. Conclusions

In this paper, we study the static behavior of a rectangular micro-plate under a constant electrostatic voltage V_{DC} and its dynamic response when subjected to electrical forces consisting of a constant voltage V_{DC} or alternating voltage V_{AC}. Nonlinear von Kármán's relations are used for developing nonlinear governing differential equations of motion for thin micro-plates which are solved by Galerkin and Multiple scale methods. The boundary conditions of the micro-plate have

Please cite this article as: I. Karimipour, Y.T. Beni and A.H. Akbarzadeh, Size-dependent nonlinear forced vibration and dynamic stability of electrically actuated micro-plates, Commun Nonlinear Sci Numer Simulat, https://doi.org/10.1016/j.cnsns.2019.104856

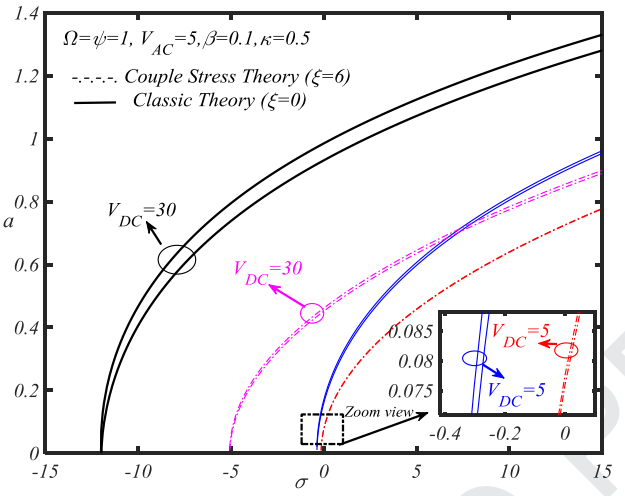

Fig. 20. The frequency response curve for a micro-plate under subharmonic resonance conditions for different V_{DC} values.

been assumed to be clamped with immovable edges. Numerical results presented in this paper leading to the following findings:

- Increasing κ (gap-to-thickness ratio) leads to an increase in the value of pull-in critical voltage and the maximum pull-in deflection of the micro-plate (Figs. 5 and 10)
- Increasing ψ (length-to-width ratio) enhances the critical electrostatic pull-in voltage and micro-plate stiffness (Fig. 6)
- It is observed that two types of critical dynamic voltage can occur in clamped micro-plates. In the first type, the micro-plate experiences a sudden fluctuation with a large amplitude (without any contact with the fixed electrode) by reaching the critical voltage. In the second type, it collides the fixed electrode due to the high vibration amplitude. In either case, the system enters an unstable region that should be avoided. (Fig. 12)
- It can be recognized that the critical dynamic voltage of clamped micro-plates is a function of the excitation force frequency for a specific DC voltage.
- It is found that the bending stiffness of the micro-plate decreases in the frequency response curve by increasing the constant DC voltage (Fig. 8). However, an increase in the alternating AC voltage does not affect the stiffness of the micro-plate (Fig. 9)

Acknowledgements

This work has been financially supported by the research deputy of Shahrekord University. The grant number was 97GRN1M835.

Appendix A: Brief Review on Modified Couple Stress Theory (MCST)

Recently, the importance of vibration at higher mode numbers besides wave propagation in wavelength at the size of the lattice of the medium attracted significant attention. So, the size effect is expected to become remarkable and from a physical point of view, the unusable of classical continuum theory in the above-mentioned cases can be demonstrated, because the wavelength approaches the scale of nanostructures and classical continuum theory fails to anticipate the size dependency [78,79]. To this end, different discrete models or continuum ones have been so far extended. Many attempts have been made to present the non-classical continuum theories by incorporating nonlocality and higher gradient of displacement in kinetic description, such as nonlocal elasticity theory, couple stress theory and strain gradient theory. Recently, studies based on these theories have been an area of active research. Although elegant, contrary to their determinative role, none of them has hitherto been provided the correct physical interpretation of characteristic length scale. Thus, it remains to be determined how the accuracy of these studies can be verified. While, the results of molecular dynamics (MDs) simulations are presented for comparison purposes, there is still controversy in results [79,80].

According to MCST, both strain and curvature tensors contribute to the strain energy density. Based on MCST, the strain energy (U) in an isotropic linear elastic material occupying region Ω can be written as [81]:

$$U = \frac{1}{2}\int_{\Omega}\left(\sigma_{ij}\varepsilon_{ij} + m_{ij}\chi_{ij}\right)\mathrm{d}\Omega \tag{A.1}$$

Please cite this article as: I. Karimipour, Y.T. Beni and A.H. Akbarzadeh, Size-dependent nonlinear forced vibration and dynamic stability of electrically actuated micro-plates, Commun Nonlinear Sci Numer Simulat, https://doi.org/10.1016/j.cnsns.2019.104856

where σ_{ij}, ε_{ij}, m_{ij} and χ_{ij} are Cauchy stress, strain, deviatoric part of couple stress tensor and symmetric curvature tensors, respectively. The constitutive relations for these tensors are defined as [82]:

$$\sigma_{ij} = \lambda\varepsilon_{ii} + 2\mu\varepsilon_{ij} \tag{A.2}$$

$$\varepsilon_{ij} = \frac{1}{2}\left(u_{i,j} + u_{j,i}\right) \tag{A.3}$$

$$m_{ij} = 2\mu l^2\ \chi_{ij} \tag{A.4}$$

$$\chi_{ij} = \frac{1}{2}\left(\theta_{i,j} + \theta_{j,i}\right) \tag{A.5}$$

where u_i is the displacement vector, $\lambda = \frac{E\upsilon}{(1+\upsilon)(1-2\upsilon)}$ and $\mu = \frac{E}{2(1+\upsilon)}$ are Lame's constants (μ is also known as shear modulus), θ_i is the rotation vector defined as Eq. (A.6) [82] and l is a material length scale parameter, which can be estimated through experimental tests [83,84], or by simulation technics such as molecular dynamics (MD), which are widely used in monitoring the behavior of a specific system of atoms during dynamic processes [85].

In comparison with other non-classical theories that have two or three parameters as length scales, modified couple stress theory by having only one length scale parameter is one the most appropriate theories in micro scale analysis. This assumption in the framework of couple stress theory might be promising and have potential applications for experimental investigations; determining only one constant via experimental methods is much easier than measuring more constants.

$$\theta_i = \frac{1}{2}e_{ijk}u_{k,j} \tag{A.6}$$

In Eq. (A.6), e_{ijk} (i, j, $k = 1, 2, 3$) represents the permutation symbol. Compared to the classical continuum mechanics, the Modified couple stress theory has one additional parameter (high-order material length scale) other than two classical Lame's constants in constitutive equations for isotropic elastic materials.

Appendix B

Hamilton's principle can be expressed as [86]:

$$\int_{t_1}^{t_2} (\delta T - \delta U + \delta W_{\text{ext}})dt = 0 \tag{B.1}$$

where δT, δU and δW_{ext} denote, virtual kinetic energy, virtual strain energy and virtual work done by external forces, respectively. The virtual kinetic energy is:

$$\begin{aligned}\delta T &= \int_Z\int_A (\rho\ddot{D}.\delta D)dAdZ \\ &= -\int_A\int_{-h/2}^{h/2}\rho\left(\frac{\partial U_1}{\partial t}\delta\frac{\partial U_1}{\partial t} + \frac{\partial V_1}{\partial t}\delta\frac{\partial V_1}{\partial t} + \frac{\partial W_1}{\partial t}\delta\frac{\partial W_1}{\partial t}\right)dZdA\end{aligned} \tag{B.2}$$

In Eq. (B.2) overdot denotes the differentiation with respect to the time variable t, and A represents the mid-plane surface and ρ is the density of micro-plate and:

$$\begin{Bmatrix} I_0 \\ I_1 \\ I_2 \end{Bmatrix} = \int_Z \rho \begin{Bmatrix} 1 \\ Z \\ Z^2 \end{Bmatrix} dZ = \rho \begin{Bmatrix} h \\ 0 \\ \frac{h^3}{12} \end{Bmatrix}, \tag{B.3}$$

$$\delta D = (\delta U - Z\delta W_{,X})\widehat{I} + (\delta V - Z\delta W_{,Y})\widehat{J} + \delta W\widehat{K}, \tag{B.4a}$$

$$\ddot{D} = \left(\ddot{U} - Z\ddot{W}_{,X}\right)\widehat{I} + \left(\ddot{V} - Z\ddot{W}_{,Y}\right)\widehat{J} + \ddot{W}\widehat{K} \tag{B.4b}$$

In equations above, D represents displacement and is defined as $D = U_1\widehat{I} + V_1\widehat{J} + W_1\widehat{K}$ and overdot denotes the differentiation concerning the time variable (t). In consideration of Eq. (A.1), the expression for virtual strain energy can be expressed as:

$$\begin{aligned}\delta U &= \int_A\int_{-h/2}^{h/2}\left\{\left(\sigma_{ij} + \sigma^r{}_{ij}\right)\delta\varepsilon_{ij} + m_{ij}\delta\chi_{ij}\right\}dZdA \\ &= \int_A\int_{-h/2}^{h/2}(\sigma_{XX}\delta\varepsilon_{XX} + \sigma_{YY}\delta\varepsilon_{YY} + \sigma_{XY}\delta\gamma_{XY} + \sigma^r_{XX}\delta\varepsilon_{XX} + \sigma^r_{YY}\delta\varepsilon_{YY} \\ &\quad + m_{XX}\delta\chi_{XX} + m_{YY}\delta\chi_{YY} + 2m_{XY}\delta\chi_{XY} + 2m_{XZ}\delta\chi_{XZ} + 2m_{ZY}\delta\chi_{ZY})dZdA\end{aligned} \tag{B.5}$$

Please cite this article as: I. Karimipour, Y.T. Beni and A.H. Akbarzadeh, Size-dependent nonlinear forced vibration and dynamic stability of electrically actuated micro-plates, Commun Nonlinear Sci Numer Simulat, https://doi.org/10.1016/j.cnsns.2019.104856

Strain energy can be written by considering Eq. (A.1):

$$U = \frac{1}{2}\times\int_{\frac{-a}{2}}^{\frac{a}{2}}\int_{\frac{-b}{2}}^{\frac{b}{2}}\int_{-\frac{h}{2}}^{\frac{h}{2}}\Im dXdYdZ,$$

$$\begin{aligned}\Im = &\left(\left\{\frac{E}{1-\upsilon^2}\left(\frac{\partial U}{\partial X}+\frac{1}{2}\left(\frac{\partial W}{\partial X}\right)^2-ZW_{,xx}+\upsilon\left(\frac{\partial V}{\partial Y}+\frac{1}{2}\left(\frac{\partial W}{\partial Y}\right)^2-ZW_{,YY}\right)\right)+\sigma_X^r\right\}\right.\\
&\times\left(\frac{\partial U}{\partial X}+\frac{1}{2}\left(\frac{\partial W}{\partial X}\right)^2-ZW_{,xx}\right)+\left(\frac{E}{1-\upsilon^2}\left(\begin{matrix}\frac{\partial V}{\partial Y}+\frac{1}{2}\left(\frac{\partial W}{\partial Y}\right)^2-ZW_{,YY}\\+\upsilon\left(\frac{\partial U}{\partial X}+\frac{1}{2}\left(\frac{\partial W}{\partial X}\right)^2-ZW_{,XX}\right)\end{matrix}\right)+\sigma_Y^r\right)\\
&\times\left(\frac{\partial V}{\partial Y}+\frac{1}{2}\left(\frac{\partial W}{\partial Y}\right)^2-ZW_{,YY}\right)+\frac{E}{2(1+\upsilon)}\left(\frac{\partial U}{\partial Y}+\frac{\partial V}{\partial X}+\frac{\partial W}{\partial X}\frac{\partial W}{\partial Y}-2ZW_{,XY}\right)^2\\
&+\frac{2El^2}{1+\upsilon}\left(\frac{\partial^2 W}{\partial X\partial Y}\right)^2+\frac{El^2}{2(1+\upsilon)}\left(\frac{\partial^2 W}{\partial Y^2}-\frac{\partial^2 W}{\partial X^2}\right)^2+\frac{El^2}{8(1+\upsilon)}\left(\frac{\partial^2 V}{\partial X^2}-\frac{\partial^2 U}{\partial X\partial Y}\right)^2\\
&\left.+\frac{El^2}{8(1+\upsilon)}\left(\frac{\partial^2 V}{\partial X\partial Y}-\frac{\partial^2 U}{\partial Y^2}\right)^2\right)\end{aligned} \tag{B.6}$$

where υ and E are the Poisson's ratio and elastic modulus of the micro-plate, respectively. The virtual work by the distributed load can be obtained as [12,13]:

$$\delta W_{\text{ext}} = \int_A f_{external}\delta W dA = \int_X\int_Y\left(\frac{\varepsilon_0 V(t)^2}{2(g-W)^2}\right)\delta W dXdY \tag{B.7}$$

In Eq. (B.7), the external force per unit area of the micro-plate, $f_{external}$, is an electric load composed of a DC component (V_{DC}) and an AC component ($V_{AC}(t)$), and ε_0 is the permittivity coefficient of vacuum, and g is the distance between these two micro-plates. Resultants of axial residual forces per unit length N_{XX}^r and N_{YY}^r are introduced as [87]:

$$N_{XX}^r = \sigma_{XX}^r h,\quad N_{YY}^r = \sigma_{YY}^r h \tag{B.8}$$

where σ_{XX}^r and σ_{YY}^r represents the axial residual stresses. Substituting Eqs. (B.2), (B.5) and (B.7) into Eq. (B.1), integrating the outcomes by parts, using the fundamental lemma of variational calculus [86] and conducting some mathematical manipulations, the following equations of motion:

$$\frac{\partial}{\partial X}\Upsilon_{XX}+\frac{\partial}{\partial Y}\Upsilon_{XY}+\frac{1}{2}\left(\frac{\partial^2}{\partial X\partial Y}\Gamma_{XZ}+\frac{\partial^2}{\partial Y^2}\Gamma_{YZ}\right)=I_0\ddot{U}, \tag{B.9a}$$

$$\frac{\partial}{\partial X}\Upsilon_{XY}+\frac{\partial}{\partial Y}\Upsilon_{YY}-\frac{1}{2}\left(\frac{\partial^2}{\partial X^2}\Gamma_{XZ}+\frac{\partial^2}{\partial X\partial Y}\Gamma_{YZ}\right)=I_0\ddot{V}, \tag{B.9b}$$

$$\begin{aligned}&\frac{\partial^2}{\partial X^2}\Xi_{XX}+2\frac{\partial^2}{\partial X\partial Y}\Xi_{XY}+\frac{\partial^2}{\partial Y^2}\Xi_{YY}+\Upsilon_{XX}\frac{\partial^2}{\partial X^2}W+2\Upsilon_{XY}\frac{\partial^2}{\partial X\partial Y}W\\
&+\Upsilon_{YY}\frac{\partial^2}{\partial Y^2}W+\frac{\partial\Upsilon_{XX}}{\partial X}\frac{\partial W}{\partial X}+\frac{\partial\Upsilon_{XY}}{\partial X}\frac{\partial W}{\partial Y}+\frac{\partial\Upsilon_{XY}}{\partial Y}\frac{\partial W}{\partial X}+\frac{\partial\Upsilon_{YY}}{\partial Y}\frac{\partial W}{\partial Y}\\
&+N_{XX}^r\frac{\partial^2 W}{\partial X^2}+N_{YY}^r\frac{\partial^2 W}{\partial Y^2}+\frac{\partial^2}{\partial X^2}\Gamma_{XY}-\frac{\partial^2}{\partial Y^2}\Gamma_{XY}+\frac{\partial^2}{\partial X\partial Y}\Gamma_{YY}-\frac{\partial^2}{\partial X\partial Y}\Gamma_{XX}\\
&+\frac{\varepsilon_0 V(t)^2}{2(g-W)^2}=I_0\ddot{W}-I_2\left(\frac{\partial^2\ddot{W}}{\partial X^2}+\frac{\partial^2\ddot{W}}{\partial Y^2}\right)\end{aligned} \tag{B.9c}$$

and boundary conditions:

$$\begin{aligned}&\left(\Upsilon_{XX}+N_{XX}^r+\frac{1}{4}\frac{\partial\Gamma_{XZ}}{\partial Y}\right)n_{XX}+\left(\Upsilon_{XY}+\frac{1}{4}\frac{\partial\Gamma_{XZ}}{\partial X}+\frac{1}{2}\frac{\partial\Gamma_{YZ}}{\partial Y}\right)n_{YY}=0\\
&\text{or}\quad \delta U=0,\end{aligned} \tag{B.10a}$$

$$\frac{1}{4}\Gamma_{XZ}n_{YY}=0\ \text{ or }\ \frac{\partial\delta U}{\partial X}=0, \tag{B.10b}$$

$$\frac{1}{4}\Gamma_{XZ}n_{XX}+\frac{1}{2}\Gamma_{YZ}n_{YY}=0\ \text{ or }\ \frac{\partial\delta U}{\partial Y}=0, \tag{B.10c}$$

Please cite this article as: I. Karimipour, Y.T. Beni and A.H. Akbarzadeh, Size-dependent nonlinear forced vibration and dynamic stability of electrically actuated micro-plates, Commun Nonlinear Sci Numer Simulat, https://doi.org/10.1016/j.cnsns.2019.104856

$$\left(\mathrm{Y}_{YY}+N^{r}_{YY}-\tfrac{1}{4}\tfrac{\partial\Gamma_{YZ}}{\partial X}\right)n_{YY}+\left(\mathrm{Y}_{XY}-\tfrac{1}{4}\tfrac{\partial\Gamma_{YZ}}{\partial Y}-\tfrac{1}{2}\tfrac{\partial\Gamma_{XZ}}{\partial X}\right)n_{XX}=0 \quad or\ \delta V=0, \tag{B.10d}$$

$$\frac{1}{4}\Gamma_{YZ}n_{YY}+\frac{1}{2}\Gamma_{XZ}n_{XX}=0 \ \ or\ \frac{\partial\delta V}{\partial X}=0, \tag{B.10e}$$

$$\frac{1}{4}\Gamma_{YZ}n_{XX}=0 \ \ or\ \frac{\partial\delta V}{\partial Y}=0, \tag{B.10f}$$

$$\begin{aligned}&\left((\mathrm{Y}_{XX}+N^{r}_{XX})\frac{\partial W}{\partial X}+(\mathrm{Y}_{XY})\frac{\partial W}{\partial Y}+\frac{\partial\Xi_{XX}}{\partial X}+\frac{\partial\Xi_{XY}}{\partial Y}\right.\\&\left.-\frac{1}{2}\frac{\partial}{\partial Y}\Gamma_{XX}+\frac{\partial}{\partial X}\Gamma_{XY}+\frac{1}{2}\frac{\partial}{\partial Y}\Gamma_{YY}+I_2\frac{\partial\ddot{W}}{\partial X}\right)n_{XX}\\&+\left((\mathrm{Y}_{YY}+N^{r}_{YY})\frac{\partial W}{\partial Y}+(\mathrm{Y}_{XY})\frac{\partial W}{\partial X}+\frac{\partial\Xi_{YY}}{\partial Y}+\frac{\partial\Xi_{XY}}{\partial X}\right.\\&\left.-\frac{1}{2}\frac{\partial}{\partial X}\Gamma_{XX}-\frac{\partial}{\partial Y}\Gamma_{XY}+\frac{1}{2}\frac{\partial}{\partial X}\Gamma_{YY}+I_2\frac{\partial\ddot{W}}{\partial Y}\right)n_{YY}=0\\&\quad or\quad \delta W=0,\end{aligned} \tag{B.10g}$$

$$(\Xi_{XX}+\Gamma_{XY})n_{XX}+\left(\Xi_{XY}-\frac{1}{2}\Gamma_{XX}+\frac{1}{2}\Gamma_{YY}\right)n_{YY}=0 \quad or\quad \frac{\partial\delta W}{\partial X}=0, \tag{B.10h}$$

$$(\Xi_{YY}-\Gamma_{XY})n_{YY}+\left(\Xi_{XY}-\frac{1}{2}\Gamma_{XX}+\frac{1}{2}\Gamma_{YY}\right)n_{XX}=0 \quad or\quad \frac{\partial\delta W}{\partial Y}=0 \tag{B.10i}$$

are derived. In above equations n_i $(i=XX,YY)$ are the components of a normal vector to the boundary of the mid-plane of micro-plate. To extract the governing equations of motion in terms of displacements, stress and couple stress consequents can be written as:

$$\begin{Bmatrix}\Xi_{XX}\\ \Xi_{YY}\\ \Xi_{XY}\end{Bmatrix}=\int_{-h/2}^{h/2}Z\begin{Bmatrix}\sigma_{XX}\\ \sigma_{YY}\\ \sigma_{XY}\end{Bmatrix}dZ=\frac{-Eh^3}{12(1-\upsilon^2)}\begin{bmatrix}1&\upsilon&0\\ \upsilon&1&0\\ 0&0&(1-\upsilon)/2\end{bmatrix}\begin{Bmatrix}\frac{\partial^2W}{\partial X^2}\\ \frac{\partial^2W}{\partial Y^2}\\ 2\frac{\partial^2W}{\partial X\partial Y}\end{Bmatrix} \tag{B.11a}$$

$$\begin{Bmatrix}\Gamma_{XX}\\ \Gamma_{YY}\\ \Gamma_{XY}\\ \Gamma_{XZ}\\ \Gamma_{YZ}\end{Bmatrix}=\int_{-h/2}^{h/2}\begin{Bmatrix}m_{XX}\\ m_{YY}\\ m_{XY}\\ m_{XZ}\\ m_{YZ}\end{Bmatrix}dZ=\frac{Ehl^2}{1+\upsilon}\begin{bmatrix}1&0&0&0&0\\ 0&-1&0&0&0\\ 0&0&-\frac{1}{2}&0&0\\ 0&0&0&-\frac{1}{4}&0\\ 0&0&0&0&-\frac{1}{4}\end{bmatrix}\begin{Bmatrix}\frac{\partial^2W}{\partial X\partial Y}\\ \frac{\partial^2W}{\partial X\partial Y}\\ \frac{\partial^2W}{\partial X^2}-\frac{\partial^2W}{\partial Y^2}\\ \frac{\partial^2U}{\partial X\partial Y}-\frac{\partial^2V}{\partial X^2}\\ \frac{\partial^2U}{\partial Y^2}-\frac{\partial^2V}{\partial X\partial Y}\end{Bmatrix} \tag{B.11b}$$

$$\begin{Bmatrix}\mathrm{Y}_{XX}\\ \mathrm{Y}_{YY}\\ \mathrm{Y}_{XY}\end{Bmatrix}=\int_{Z}\begin{Bmatrix}\sigma_{XX}\\ \sigma_{YY}\\ \sigma_{XY}\end{Bmatrix}dZ=\frac{Eh}{(1-\upsilon^2)}\begin{bmatrix}1&\upsilon&0\\ \upsilon&1&0\\ 0&0&(1-\upsilon)/2\end{bmatrix}\begin{Bmatrix}\frac{\partial U}{\partial X}+\frac{1}{2}\left(\frac{\partial W}{\partial X}\right)^2\\ \frac{\partial V}{\partial Y}+\frac{1}{2}\left(\frac{\partial W}{\partial Y}\right)^2\\ \frac{\partial U}{\partial Y}+\frac{\partial V}{\partial X}+\frac{\partial W}{\partial X}\frac{\partial W}{\partial Y}\end{Bmatrix} \tag{B.11c}$$

Appendix C

Constant C_1, C_2, A_n, and B_n, introduced in Eq. (36), are determined here. On the determination of these constants, it is observed that:

$$[F_{c,XY}]_{X=\pm a/2}=Eg^2{W_m}^2\sum_{n=1}^{n}\frac{\mp 2An\pi\,\sin(n\pi)\lambda}{na(U\lambda P+n\pi)}\left(-2\frac{\pi Un(2\pi nYQ+aR)}{a^2}\right.$$

Please cite this article as: I. Karimipour, Y.T. Beni and A.H. Akbarzadeh, Size-dependent nonlinear forced vibration and dynamic stability of electrically actuated micro-plates, Commun Nonlinear Sci Numer Simulat, https://doi.org/10.1016/j.cnsns.2019.104856

$$+2\frac{n\pi\,(P\pi\,n+U\lambda)R}{a\lambda}\Bigg)-\frac{2BTn\pi}{\lambda^2 nb(\sinh(n\pi\,\lambda)\cosh(n\pi\,\lambda)+n\pi\,\lambda)}$$
$$\times\Bigg(\pm2\frac{(\sinh(n\pi\,\lambda)+n\pi\,\lambda\cosh(n\pi\,\lambda))n\pi\,\sinh(K)}{b}+$$
$$\frac{(\mp2\sinh(n\pi\,\lambda)\cosh(K)K\mp2\sinh(n\pi\,\lambda)\sinh(K))n\pi}{b}\Bigg),$$
$$[F_{c,XY}]_{Y=\pm b/2}=\sum_{n=1}^{n}\pm4\frac{Eg^2{W_m}^2Bnn\pi^3\sin(n\pi)}{b^3\lambda^2(\sinh(n\pi\,\lambda)\cosh(n\pi\,\lambda)+n\pi\,\lambda)}$$
$$\times\Bigg(-\cosh(n\pi\,\lambda)\sinh\left(2\frac{n\pi X}{b}\right)b\lambda+2\sinh(n\pi\,\lambda)HX\Bigg)$$
$$-\frac{2An\pi\,\lambda J}{na(U\lambda P+n\pi)}\Bigg(\pm2\frac{n\pi\,\sinh(S)(P\pi\,n+U\lambda)}{a\lambda}\mp$$
$$2\frac{\pi Un(\pi\,\cosh(S)bn+\sinh(S)a)}{a^2}\Bigg) \tag{C.1}$$

where

$$H=\cosh(2\frac{n\pi X}{b}),\ S=\frac{n\pi\,b}{a},\ T=\sin\left(2\frac{n\pi Y}{b}\right),\ \mathrm{P}=\cosh\left(\frac{n\pi}{\lambda}\right),$$
$$\mathrm{U}=\sinh\left(\frac{n\pi}{\lambda}\right),\ K=\frac{n\pi\,a}{b},\quad Q=\cosh(2\frac{n\pi Y}{a}),\ \mathrm{R}=\sinh(2\frac{n\pi Y}{a}) \tag{C.2}$$

Introducing equation $F=F_c+F_p$ into the equation of boundary conditions (18) and taking into account Eqs. (35) and (C.2), the constants C_1 *and* C_2 are determined.

Appendix D

The coefficients $A_i,\ \ i=1,2,\ldots,8$, of Eq. (56) are presented as:

$$A_1=-\frac{25}{18},A_2=\frac{1225}{2304},A_3=16/3\left(\begin{matrix}\left(\psi^4+2/3\psi^2+1\right)(\xi+1)\pi^2\\+1/4\psi^2N_y+N_x/4\end{matrix}\right)\pi^2,$$
$$A_4=-\frac{80\pi^2\left(\left(\psi^4+4/5\psi^2+1\right)(\xi+1)\pi^2+1/4\psi^2N_y+N_x/4\right)}{9},$$
$$A_8=-\frac{16\beta\,(V_{DC}+V_{AC}\cos(\Omega t))^2}{9},$$
$$A_6=\frac{\begin{matrix}(\upsilon+1)\pi^4\left(264\psi^{16}\upsilon-504\psi^{16}+2772\psi^{14}\upsilon-5532\psi^{14}+11267\psi^{12}\upsilon\right.\\-22922\psi^{12}+24218\psi^{10}\upsilon-47063\psi^{10}+34158\psi^8\upsilon-57003\psi^8\\+24218\psi^6\upsilon-35873\psi^6+11267\psi^4\upsilon-14027\psi^4+2772\psi^2\upsilon\\\left.-3012\psi^2+264\upsilon-264\right)\kappa^2\end{matrix}}{96\left(\psi^2+1/4\right)^2\left(\psi^2+1\right)^2\left(\psi^2+4\right)^2}, \tag{D.1}$$

$$A_7=-\frac{\begin{matrix}(21\upsilon+21)\pi^4\left(480\psi^{16}\upsilon-880\psi^{16}+5040\psi^{14}\upsilon-9640\psi^{14}\right.\\+20846\psi^{12}\upsilon-40271\psi^{12}+45740\psi^{10}\upsilon-83815\psi^{10}+65388\psi^8\upsilon\\-103463\psi^8+45740\psi^6\upsilon-65165\psi^6+20846\psi^4\upsilon-25446\psi^4+\\\left.5040\psi^2\upsilon-5440\psi^2+480\upsilon-480\right)\kappa^2\end{matrix}}{8192\left(\psi^2+1/4\right)^2\left(\psi^2+1\right)^2\left(\psi^2+4\right)^2}$$

Please cite this article as: I. Karimipour, Y.T. Beni and A.H. Akbarzadeh, Size-dependent nonlinear forced vibration and dynamic stability of electrically actuated micro-plates, Commun Nonlinear Sci Numer Simulat, https://doi.org/10.1016/j.cnsns.2019.104856

$$A_5 = \frac{\left(\left(\left(\frac{786}{175} - \frac{102\upsilon^2}{25} + \frac{72\upsilon}{175}\right)\kappa^2 + \frac{159}{14} + \frac{159\xi}{14}\right)\pi^2 + \frac{21N_x}{8} + N_y/4\right)\psi^2\right\}}{48\left(\psi^2+4\right)^2\left(\psi^2+1\right)^2\left(\psi^2+1/4\right)^2}$$

$$\begin{aligned}
&175\pi^2 \times \left\{\left(\left(\tfrac{4}{5} - \tfrac{68\upsilon^2}{175} + \tfrac{72\upsilon}{175}\right)\kappa^2 + \xi + 1\right)\pi^2\psi^{16} + \left(\left(\tfrac{68}{175} - \tfrac{68\upsilon^2}{175}\right)\kappa^2 + \xi + 1\right)\pi^2\right.\\
&+N_x/4 + \left(\left(-\tfrac{(102\upsilon+102)\kappa^2}{25}\left(\upsilon - \tfrac{257}{119}\right) + \tfrac{159}{14} + \tfrac{159\xi}{14}\right)\pi^2 + N_y/4\right)\psi^{14} +\\
&\left(\left(\left(\tfrac{25259}{700} - \tfrac{11273\upsilon^2}{700} + \tfrac{999\upsilon}{50}\right)\kappa^2 + \tfrac{769}{16} + \tfrac{769\xi}{16}\right)\pi^2 + N_x/4 + \tfrac{21N_y}{8}\right)\psi^{12} +\\
&\left(\left(\left(\tfrac{2528}{35} - \tfrac{11573\upsilon^2}{350} + \tfrac{13707\upsilon}{350}\right)\kappa^2 + \tfrac{401}{4} + \tfrac{401\xi}{4}\right)\pi^2 + \tfrac{21N_x}{8} + \tfrac{609N_y}{64}\right)\psi^{10} + \psi^8\\
&\left(-\tfrac{(15753\upsilon+15753)\kappa^2\left(\upsilon - \frac{9820}{5251}\right)}{350} + \tfrac{7005+7005\xi}{56}\right)\pi^2 + \tfrac{609N_x+914N_y}{64}\\
&+\left(\left(\left(\tfrac{9283}{175} - \tfrac{11573\upsilon^2}{350} + \tfrac{999\upsilon}{50}\right)\kappa^2 + \tfrac{401}{4} + \tfrac{401\xi}{4}\right)\pi^2 + \tfrac{457N_x}{32} + \tfrac{609N_y}{64}\right)\psi^6\\
&+\left(\left(\left(\tfrac{2917}{140} - \tfrac{11273\upsilon^2}{700} + \tfrac{828\upsilon}{175}\right)\kappa^2 + \tfrac{769}{16} + \tfrac{769\xi}{16}\right)\pi^2 + \tfrac{609N_x}{64} + \tfrac{21N_y}{8}\right)\psi^4 +
\end{aligned}$$

It is worth mentioning that, we assume in the abovementioned equations that voltage varies according to $V(t) = V_{DC} + V_{AC}\cos(\Omega t)$, Ω is the excitation frequency

References

[1] Francais O, Dufour I. Normalized abacus for the global behavior of diaphragms: pneumatic, electrostatic, piezoelectric or electromagnetic actuation. J Model Simul Microsyst 1999;2:149–60.
[2] Ghayesh MH, Farokhi H. Nonlinear behaviour of electrically actuated microplate-based MEMS resonators. Mech Syst Signal Process 2018;109:220–34.
[3] Farokhi H, Ghayesh MH. On the dynamics of imperfect shear deformable microplates. Int J Eng Sci 2018;133:264–83.
[4] Batra R, Porfiri M, Spinello D. Review of modeling electrostatically actuated microelectromechanical systems. Smart Mater Struct 2007;16:R23.
[5] Shojaeian M, Beni YT. Size-dependent electromechanical buckling of functionally graded electrostatic nano-bridges. Sens Actuators, A 2015;232:49–62.
[6] Tadi Beni Y. Size-dependent electromechanical bending, buckling, and free vibration analysis of functionally graded piezoelectric nanobeams. J Intell Mater Syst Struct 2016;27:2199–215.
[7] Akbarzadeh A, Pasini D. Multiphysics of multilayered and functionally graded cylinders under prescribed hygrothermomagnetoelectromechanical loading. J Appl Mech 2014;81:041018.
[8] Akbarzadeh A, Chen Z. Hygrothermal stresses in one-dimensional functionally graded piezoelectric media in constant magnetic field. Compos Struct 2013;97:317–31.
[9] Belardinelli P, Sajadi B, Lenci S, Alijani F. Global dynamics and integrity of a micro-plate pressure sensor. Commun Nonlinear Sci Numer Simul 2019;69:432–44.
[10] Akbarzadeh A, Chen Z. Thermo-magneto-electro-elastic responses of rotating hollow cylinders. Mech Adv Mater Struct 2014;21:67–80.
[11] Francais O, Dufour I. Dynamic simulation of an electrostatic micropump with pull-in and hysteresis phenomena. Sens Actuators, A 1998;70:56–60.
[12] Hayt WH, Buck JA. Engineering electromagnetics. New York: McGraw-Hill; 2001.
[13] Karimipour I, Beni YT, Zeighampour H. Nonlinear size-dependent pull-in instability and stress analysis of thin plate actuator based on enhanced continuum theories including nonlinear effects and surface energy. Microsyst Technol 2018;24:1811–39.
[14] Sajadi B, Alijani F, Goosen H, van Keulen F. Effect of pressure on nonlinear dynamics and instability of electrically actuated circular micro-plates. Nonlinear Dyn 2018;91:2157–70.
[15] Bourouina T, Grandchamp J-P. Modeling micropumps with electrical equivalent networks. J Micromech Microeng 1996;6:398.
[16] Cozma A, Puers R. Electrostatic actuation as a self-testing method for silicon pressure sensors. Sens Actuators, A 1997;60:32–6.
[17] Saif M, Alaca BE, Sehitoglu H. Analytical modeling of electrostatic membrane actuator for micro pumps. J Microelectromech Syst 1999;8:335–45.
[18] Yang F. Electromechanical instability of microscale structures. J Appl Phys 2002;92:2789–94.
[19] Rajalingham C, Bhat R. Influence of an electric field on diaphragm stability and vibration in a condenser microphone. J Sound Vib 1998;211:819–27.
[20] Zook J, Burns D, Guckel H, Sniegowski J, Engelstad R, Feng Z. Characteristics of polysilicon resonant microbeams. Sens Actuators, A 1992;35:51–9.
[21] Choi B, Lovell E. Improved analysis of microbeams under mechanical and electrostatic loads. J Micromech Microeng 1997;7:24.
[22] Ahn Y, Guckel H, Zook JD. Capacitive microbeam resonator design. J Micromech Microeng 2001;11:70.
[23] Tilmans HA, Legtenberg R. Electrostatically driven vacuum-encapsulated polysilicon resonators: part II. Theory and performance. Sens Actuators, A 1994;45:67–84.
[24] Ayela F, Fournier T. An experimental study of anharmonic micromachined silicon resonators. Meas Sci Technol 1998;9:1821.
[25] Veijola T, Mattila T, Jaakkola O, Kiihamaki J, Lamminmaki T, Oja A, et al. Large-displacement modelling and simulation of micromechanical electrostatically driven resonators using the harmonic balance method. In: Proceedings of the Microwave Symposium Digest 2000 IEEE MTT-S International. IEEE; 2000. p. 99–102.
[26] Konig E, Wachutka G. Analysis of unstable behavior occurring in electro-mechanical microdevices. In: Proceedings of the Modeling Simulation of Microsystems; 1999. p. 330–3.
[27] Sedighi HM, Koochi A, Daneshmand F, Abadyan M. Non-linear dynamic instability of a double-sided nano-bridge considering centrifugal force and rarefied gas flow. Int J Non Linear Mech 2015;77:96–106.
[28] Ng T, Jiang T, Li H, Lam K, Reddy J. A coupled field study on the non-linear dynamic characteristics of an electrostatic micropump. J Sound Vib 2004;273:989–1006.
[29] Zhao X, Abdel-Rahman EM, Nayfeh AH. A reduced-order model for electrically actuated microplates. J Micromech Microeng 2004;14:900.
[30] Nayfeh AH, Pai PF. Linear and nonlinear structural mechanics. John Wiley & Sons; 2008.
[31] Sarvestani HY, Akbarzadeh A, Mirabolghasemi A. Structural analysis of size-dependent functionally graded doubly-curved panels with engineered microarchitectures. Acta Mech 2018;229:2675–701.
[32] Taati E, Najafabadi MM, Reddy J. Size-dependent generalized thermoelasticity model for Timoshenko micro-beams based on strain gradient and non-fourier heat conduction theories. Compos Struct 2014;116:595–611.
[33] Fatikow S, Rembold U. Microsystem technology and microrobotics. Springer Science & Business Media; 2013.
[34] Beni YT, Karimipour I, Abadyan M. Modeling the instability of electrostatic nano-bridges and nano-cantilevers using modified strain gradient theory. Appl Math Model 2015;39:2633–48.
[35] Karimipour I, Beni YT, Koochi A, Abadyan M. Using couple stress theory for modeling the size-dependent instability of double-sided beam-type nanoactuators in the presence of Casimir force. J Braz Soc Mech Sci Eng 2016;38:1779–95.
[36] Beni YT, Karimipöur I, Abadyan M. Modeling the effect of intermolecular force on the size-dependent pull-in behavior of beam-type NEMS using modified couple stress theory. J Mech Sci Technol 2014;28:3749–57.
[37] Eringen AC, Edelen D. On nonlocal elasticity. Int J Eng Sci 1972;10:233–48.
[38] Eringen AC. Theory of micropolar elasticity. In: Microcontinuum field theories. Springer; 1999. p. 101–248.

Please cite this article as: I. Karimipour, Y.T. Beni and A.H. Akbarzadeh, Size-dependent nonlinear forced vibration and dynamic stability of electrically actuated micro-plates, Commun Nonlinear Sci Numer Simulat, https://doi.org/10.1016/j.cnsns.2019.104856

[39] Karimipour I, Kanani A, Koochi A, Keivani M, Abadyan M. Modeling the electromechanical behavior and instability threshold of NEMS bridge in electrolyte considering the size dependency and dispersion forces. Phys E 2015;74:140–50.
[40] Sedighi HM. Size-dependent dynamic pull-in instability of vibrating electrically actuated microbeams based on the strain gradient elasticity theory. Acta Astronaut 2014;95:111–23.
[41] Shojaeian M, Beni YT, Ataei H. Electromechanical buckling of functionally graded electrostatic nanobridges using strain gradient theory. Acta Astronaut 2016;118:62–71.
[42] Ghobadi A, Beni YT, Golestanian H. Size dependent thermo-electro-mechanical nonlinear bending analysis of flexoelectric nano-plate in the presence of magnetic field. Int J Mech Sci 2019;152:118–37.
[43] Hamilton J, Wolfer W. Theories of surface elasticity for nanoscale objects. Surf Sci 2009;603:1284–91.
[44] Sedighi HM, Bozorgmehri A. Dynamic instability analysis of doubly clamped cylindrical nanowires in the presence of Casimir attraction and surface effects using modified couple stress theory. Acta Mech 2016;227:1575–91.
[45] Tsiatas GC. A new Kirchhoff plate model based on a modified couple stress theory. Int J Solids Struct 2009;46:2757–64.
[46] Yin L, Qian Q, Wang L, Xia W. Vibration analysis of microscale plates based on modified couple stress theory. Acta Mech Solida Sin 2010;23:386–93.
[47] Jomehzadeh E, Noori H, Saidi A. The size-dependent vibration analysis of micro-plates based on a modified couple stress theory. Phys. E 2011;43:877–83.
[48] Asghari M. Geometrically nonlinear micro-plate formulation based on the modified couple stress theory. Int J Eng Sci 2012;51:292–309.
[49] Wang Y-G, Lin W-H, Zhou C-L. Nonlinear bending of size-dependent circular microplates based on the modified couple stress theory. Arch Appl Mech 2014;84:391–400.
[50] Akgöz B, Civalek Ö. Modeling and analysis of micro-sized plates resting on elastic medium using the modified couple stress theory. Meccanica 2013;48:863–73.
[51] Askari AR, Tahani M. Analytical determination of size-dependent natural frequencies of fully clamped rectangular microplates based on the modified couple stress theory. J Mech Sci Technol 2015;29:2135–45.
[52] Askari AR, Tahani M. Size-dependent dynamic pull-in analysis of geometric non-linear micro-plates based on the modified couple stress theory. Phys E 2017;86:262–74.
[53] Tahani M, Askari AR, Mohandes Y, Hassani B. Size-dependent free vibration analysis of electrostatically pre-deformed rectangular micro-plates based on the modified couple stress theory. Int J Mech Sci 2015;94:185–98.
[54] Zhang B, He Y, Liu D, Gan Z, Shen L. A non-classical Mindlin plate finite element based on a modified couple stress theory. Eur J Mech A/Solids 2013;42:63–80.
[55] Ansari R, Shojaei MF, Mohammadi V, Gholami R, Darabi M. Nonlinear vibrations of functionally graded Mindlin microplates based on the modified couple stress theory. Compos Struct 2014;114:124–34.
[56] Lou J, He L. Closed-form solutions for nonlinear bending and free vibration of functionally graded microplates based on the modified couple stress theory. Compos Struct 2015;131:810–20.
[57] Thai H-T, Choi D-H. Size-dependent functionally graded Kirchhoff and Mindlin plate models based on a modified couple stress theory. Compos Struct 2013;95:142–53.
[58] Thai H-T, Kim S-E. A size-dependent functionally graded Reddy plate model based on a modified couple stress theory. Compos Part B Eng 2013;45:1636–45.
[59] Thai H-T, Vo TP. A size-dependent functionally graded sinusoidal plate model based on a modified couple stress theory. Compos Struct 2013;96:376–83.
[60] Reddy JN. Mechanics of laminated composite plates and shells: theory and analysis. CRC press; 2004.
[61] Reddy JN. Theory and analysis of elastic plates and shells. CRC press; 2006.
[62] Nayfeh AH, Mook DT. Nonlinear oscillations. John Wiley & Sons; 2008.
[63] Alijani F, Amabili M. Effect of thickness deformation on large-amplitude vibrations of functionally graded rectangular plates. Compos Struct 2014;113:89–107.
[64] Alijani F, Amabili M. Nonlinear vibrations of laminated and sandwich rectangular plates with free edges. Part 1: theory and numerical simulations. Compos Struct 2013;105:422–36.
[65] Younis MI. MEMS linear and nonlinear statics and dynamics. Springer Science & Business Media; 2011.
[66] Zietlow DW, Griffin DC, Moore TR. The limitations on applying classical thin plate theory to thin annular plates clamped on the inner boundary. AIP Adv 2012;2:042103.
[67] Yamaki N. Influence of large amplitudes on flexural vibrations of elastic plates. ZAMM J Appl Math Mech Z für Angew Math und Mech 1961;41:501–10.
[68] Kung G, Pao Y-H. Nonlinear flexural vibrations of a clamped circular plate. J Appl Mech 1972;39:1050–4.
[69] Hadian J, Nayfeh A. Modal interaction in circular plates. J Sound Vib 1990;142:279–92.
[70] Shi Y, Mei C. A finite element time domain modal formulation for large amplitude free vibrations of beams and plates. J Sound Vib 1996;193:453–64.
[71] Benamar R, Bennouna M, White R. The effects of large vibration amplitudes on the mode shapes and natural frequencies of thin elastic structures, part II: fully clamped rectangular isotropic plates. J Sound Vib 1993;164:295–316.
[72] Amabili M. Nonlinear vibrations and stability of shells and plates. Cambridge University Press; 2008.
[73] Chia C-Y. Nonlinear analysis of plates. McGraw-Hill International Book Company; 1980.
[74] Farokhi H, Ghayesh MH. Supercritical nonlinear parametric dynamics of Timoshenko microbeams. Commun Nonlinear Sci Numer Simul 2018;59:592–605.
[75] Ghayesh MH. Dynamical analysis of multilayered cantilevers. Commun Nonlinear Sci Numer Simul 2019;71:244–53.
[76] Yeh F, Liu W. Nonlinear analysis of rectangular orthotropic plates. Int J Mech Sci 1991;33:563–78.
[77] Suleiman OME. Nonlinear analysis of rectangular laminated plates, Germany: Lap Lambert Academic Publishing; 2015. ISBN:(978-3-659-76787-6).
[78] Ma H, Gao X-L, Reddy J. A microstructure-dependent Timoshenko beam model based on a modified couple stress theory. J Mech Phys Solids 2008;56:3379–91.
[79] Nejad MZ, Hadi A, Rastgoo A. Buckling analysis of arbitrary two-directional functionally graded Euler–Bernoulli nano-beams based on nonlocal elasticity theory. Int J Eng Sci 2016;103:1–10.
[80] Askes H, Aifantis EC. Gradient elasticity in statics and dynamics: an overview of formulations, length scale identification procedures, finite element implementations and new results. Int J Solids Struct 2011;48:1962–90.
[81] Yang F, Chong A, Lam DCC, Tong P. Couple stress based strain gradient theory for elasticity. Int J Solids Struct 2002;39:2731–43.
[82] Reddy J, Kim J. A nonlinear modified couple stress-based third-order theory of functionally graded plates. Compos Struct 2012;94:1128–43.
[83] Hadjesfandiari, AR, Hajesfandiari, A, Dargush, GF. Pure plate bending in couple stress theories, arXiv: 160602954 (2016).
[84] Hadjesfandiari, AR, Dargush, GF. An assessment of higher gradient theories from a continuum mechanics perspective, arXiv: 181006977 (2018).
[85] Rafii-Tabar H, Shodja H, Darabi M, Dahi A. Molecular dynamics simulation of crack propagation in FCC materials containing clusters of impurities. Mech Mater 2006;38:243–52.
[86] Reddy JN. Energy principles and variational methods in applied mechanics. John Wiley & Sons; 2017.
[87] SHAH, MAA, Rezazadeh, G, Shabani, R. Effect of electric potential distribution on electromechanical behavior of a piezoelectrically sandwiched micro-beam. (2012).

Please cite this article as: I. Karimipour, Y.T. Beni and A.H. Akbarzadeh, Size-dependent nonlinear forced vibration and dynamic stability of electrically actuated micro-plates, Commun Nonlinear Sci Numer Simulat, https://doi.org/10.1016/j.cnsns.2019.104856